# 國 立 清 華 大 學

# National Tsing Hua University

## 碩 士 論 文

## Master Thesis

低能有效框架下的玻色子：自子衰及更的束

Low Energy EFT Framework for Charged Boson Portals:
Constraints from Lepton Decays and Beyond


系別：物理系 Department of Physics

學號：110022421

研 究 生：黎德傳 Duc Truyen LE

指導教授：張維甫 We-Fu CHANG



中 華 民 國 一一二 年 一〇 月

R.O.C. 112-10

# Abstract

This study presents a detailed construction of a low energy Effective Field Theory (EFT) framework that introduces novel charged bosons potentially deemed to be the SM and Dark sector portals. The newly charged mediators have coupling to photon and generally arbitrary couplings to fermions, both matter and dark matter particles, which therefore significantly contribute to hugely vast experimental processes. That adjusts the theoretical prediction of experimental values, particularly lepton decays within the scope of our study. Preliminary to this theoretical development is the verification of the anapole moment's disappearance at the one-loop order, guaranteeing its gauged invariant Lagrangian. By employing lepton decays, we impose constraints on the newly introduced couplings. A pivotal aspect of our analysis involves the use of Michel parameters [1, 2] derived from polarized muon decay, which plays a key role in assessing the chirality effects predicted by the theory. Our findings indicate that the proposed couplings are too constrained to explain the muon g-2 anomaly if a universal coupling assumption is made. In addition, the given coupling pattern of UV models can also be applied to offer a better lower bound of detecting charged boson mass than collider searches that surpass and/or benchmarks with other current experimental searches. Last but most importantly, the work addressed the rigorous constraints arising further from Lepton Flavor Violation decays and Neutrino Oscillation within the Zee Model context. Utilizing Michel parameters showcased an impactful point, which set out the comprehensive analysis of limiting parameter space for the Zee model to survive compared to other previous research works. The findings of this study provide a framework analysis for exploring new physics in the weak sector and offer a significant step forward in resolving longstanding anomalies in particle physics.

# Contents

# List of Figures

# List of Tables

# Chapter 1

# Introduction

**Motivation why the mass range 10-100 GeV**

- low mass scale causes the low magnitude of coupling compared to $G_F$ also gives a large contribution to $a_l$
- Can not be too small due to long-range interaction and cosmological formation constraints. Additionally, our concern scale must be $> m_\mu$
- be excluded by exp.

**In the quest to understand the fundamental constituents of nature, Effective Field Theory (EFT) has emerged as a powerful conceptual and mathematical framework, enabling physicists to systematically investigate the implications of these experimental findings. EFT allows physicists to focus on the relevant degrees of freedom at a given energy scale, effectively encapsulating the ignorance about higher energy physics by integrating higher-dimensional operators that encloses potential new physics into the EFT model. This approach has been instrumental in providing systematic expansions when dealing with physical systems characterized by a separation of scales.

One of the persistent challenges in particle physics is the hierarchy problem, which concerns the vast difference between the gravitational scale and the electroweak scale. This problem often motivates the introduction of new particles and symmetries to stabilize the Higgs mass against radiative corrections. In this context, we explore the possibility of extending the Standard Model (SM) with additional particles that carry electric charge and thus participate in electromagnetic interactions, governed by the $\mathrm{U}(1)_{\mathrm{EM}}$ gauge symmetry.

The $\mathrm{U}(1)_{\mathrm{EM}}$ symmetry, a cornerstone of the SM, dictates the dynamics of charged particles and their interactions with the photon. Any extension of the SM must respect this symmetry to remain consistent with the well-established electromagnetic phenomena.

Previous attempts to introduce new particles into the EFT framework have provided valuable insights but also raised new questions. For instance, the introduction of heavy vector-like quarks and leptons has been studied extensively, but their integration into a coherent EFT that respects gauge symmetries and is renormalizable remains a challenge.

In this work, we propose a novel EFT model that introduces a new charged vector boson and a new charged scalar. These particles are coupled in a manner that is renormalizable and invariant under $\mathrm{U}(1)_{\mathrm{EM}}$ symmetry. The renormalizable coupling introduced here is designed to ensure that the new particles can be consistently incorporated into the EFT without introducing anomalies or breaking gauge invariance.**

The structure of this thesis is as follows: Chapter 2 provides a detailed construction of EFT respecting the low-energy symmetry. Chapters 3 and 4 discuss the theoretical footings of the EFT underlying Michel parameters and the leptonic decays's phenomenology study. In Chapter 5, we investigate the boundary constraint of new charged bosons and explore their potential solution for the $g-2$ problem via Michel parameters. Chapter 6 presents a detailed application of the triplet Higgs model and provides an upper bound for the Yukawa couplings. Finally, Chapter 7 offers conclusions and perspectives for future research. In the realm of Lepton Flavor Violation, the constraints placed by this study will guide future experiments and theories, potentially leading to novel discoveries or the refinement of existing models,

# Chapter 2

# Effective Field Theory model

**Effective Field Theory (EFT) acknowledges the constraints of our understanding, accepting that our theories are simplified representations of a reality much more intricate than we currently comprehend. Yet, it also embodies our determination to not be hindered by these constraints. Rather than pursuing an unattainable, all-inclusive theory, EFT enables us to develop models that are effective within certain scales, utilizing the known elements to investigate the yet-to-be-discovered aspects

This is the bottom-up approach, where we start with what we observe and carefully, piece by piece, build our models to higher energies and smaller scales. Each effective theory is a rung on a ladder stretching into the heavens of high-energy physics. We may not see the top of this ladder, but with each step, we rise higher, see farther, and understand more.

In this chapters to come, we will explore the elegance of EFT, a framework that allows us to approximate the unknown using the language of the known. We will celebrate the victories of past discoveries and set our sights on the horizons of the future. This is not just the story of EFT; it is the story of human curiosity, our relentless pursuit of truth, and the unyielding hope that in the fabric of the cosmos, we will find our place in the grand pattern.**

EFT building procedure from the bottom-up point of view. Apart from the typical approach in which we add non-renormalizable contributions along with the UV regulator $\frac{1}{\Lambda}$, where $\Lambda$ is a new physics mass scale. Herein, we introduce renormalizable couplings along with new particles coupling to SM particles, which is what happens in Higg sector development. In this chapter, we go about setting up an EFT Lagrangian, which describes the presence of new charged boson particles

## 2.1 Charged vector boson

To construct an EFT Lagrangian with a new charged vector boson, we have to satisfy conventionally fundamental symmetries and invariances, at the low-energy scale, these are typically Lorentz invariance and $U(1)_{\mathrm{EM}}$ group. In the first step, we bring in the kinetic term of charged vector field $V^{\pm}_{\mu\nu} \equiv \partial_\mu V^{\pm}_{\nu} - \partial_\nu V^{\pm}_{\mu}$ in free interaction obeying Lorentz invariance

$$\mathcal{L}_{V^\pm} = \epsilon V^{+}_{\mu\nu} V^{-\mu\nu} + m^2 V^{+}_{\mu} V^{-\mu}, \tag{2.1}$$

where the factor magnitude is defined through E.O.M reduced to the Klein-Gordon equation

$$\partial_\mu \frac{\partial \mathcal{L}_{V^\pm}}{\partial(\partial_\mu V^{\pm}_{\nu})} - \frac{\partial \mathcal{L}_{V^\pm}}{\partial V^{\pm}_{\nu}} = 2a\partial^\nu V^{\pm}_{\mu\nu} + m^2 V^{\pm}_{\mu} = 0, \tag{2.2}$$

we obtain the Lorentz gauge condition $\partial^\mu V^{\pm}_{\mu} = 0$ by taking derivative $\partial^\mu$ to E.O.M. Consequently, to derive the relativistic Schrödinger equation for charged vector field, we set $\epsilon = -\frac{1}{2}$

$$2\epsilon\partial^\nu \left(\partial_\mu V^{\pm}_{\nu} - \partial_\nu V^{\pm}_{\mu}\right) + m^2 V^{\pm}_{\mu} = \left(-2\epsilon\partial^\nu\partial_\nu + m^2\right) V^{\pm}_{\mu} = \left(\Box + m^2\right) V^{\pm}_{\mu} = 0. \tag{2.3}$$

The relative sign between $m^2$ and $\epsilon$ is defined by the positive definite of energy

$$\mathcal{E} = \frac{\partial \mathcal{L}_{V^\pm}}{\partial\left(\partial_t V_\mu^\pm\right)}\partial_t V_\mu^\pm - \mathcal{L}_{V^\pm} = -V^{\mp,0\mu}\partial_t V_\mu^\pm + \frac{1}{2}V_{\mu\nu}^+ V^{-\mu\nu} - m^2 V_\mu^+ V^{-\mu} \tag{2.4}$$

$$= \partial_i V_0^\pm \partial_0 V_i^\mp - \partial_i V_0^+ \partial_i V_0^- - m^2\left(V_0^+ V_0^- - V_i^+ V_i^-\right) \tag{2.5}$$

$$= \left(\partial_i V_0^\pm \partial_0 V_i^\mp + V_0^\pm \partial_0^2 V_0^\mp\right) - V_0^\pm\left(\Box + m^2\right)V_0^\mp + m^2 V_i^+ V_i^- \tag{2.6}$$

$$= m^2 V_i^+ V_i^- \geq 0. \tag{2.7}$$

Here, we ignored the total derivative terms $\partial_i\hat{\mathcal{O}}$ which has no effect on total energy after integration, and used the Klein-Gordon equation along with Lorentz gauge condition to extract Eq. 2.6 to Eq. 2.7. Indeed, the Lorentz gauge is used to constrain the Lorentz representation spin-zero component in the vector field, and in order to impose that such condition, the relative factor between $\partial_\mu V_\nu^\pm \partial^\mu V^{\mp\nu}$ and $\partial_\mu V_\nu^\pm \partial^\nu V^{\mp\mu}$ is fixed, subsequently, $F_{\mu\nu}^\pm$ was then formed.

The second step involves interaction with the gauge field, especially photon, the standard procedure is that we convert the normal partial derivative to covariant derivative $\partial_\mu \to D_\mu = \partial_\mu + ieQ_V A_\mu$, the photon field $A_\mu$ here basically played a role as an affine connection between two points in complex field space. Interestingly, it is not the end of our story, there is another photon interaction term that we can also include in our model, which basically exerts a contribution to the MDM effect

$$\mathcal{L}_{\text{int}} \supset aieQ_V F^{\mu\nu} V_\mu^+ V_\nu^-, \tag{2.8}$$

with factor $\underline{a}$ is a "free" real number due to the antisymmetric photon field tensor $F^{\mu\nu}$. This is a mysterious emergence while we expected the full coupling with the photon field should be induced through the covariant derivative. In SM, $V^\pm$ is indeed the $W^\pm$ boson, and this bizarre effect originates from non-abelian properties and the connately neutral vector boson coming along with the charged one. To sustain the covariant derivative-based method and resolve the anomaly, hence, the neutral vector boson would do the job, nevertheless, we will not consider that and assume only the new charged boson appears. One more legit term is the quartic potential of $V_\mu^\pm$, such as $b|V_\mu^\pm|^4$, which we also ignored here thanks to its non-contribution to our relevant process.

Crucially, the coefficient $\underline{a}$ in Eq. 2.8 must be fixed as a constant to ensure convergence of the magnetic dipole moment. The proper selection of $\underline{a}$ avoids the divergence that would otherwise arise in the calculation of the MDM, a detailed address of this issue and proof within the context of this effective theory will be the subject of a discussion in Chapter 4. Therein, we will pinpoint the necessity of the contribution Eq. 2.8 for the renormalization of the MDM and its complementary role in the EFT framework, ensuring that the predictions of our model remain physically meaningful.

In the final step of our consideration, we formalize the interaction Lagrangian representing the dynamics between the charged vector bosons and the fermionic matter fields. This interaction is crucial, as it, in general, encapsulates the effects we aim to investigate, particularly those pertaining to the chiral properties of the weak force.

$$\mathcal{L}_{\text{int}} \supset \bar{\psi}_i \left( V_{ij}^L \hat{L} + V_{ij}^R \hat{R} \right) \gamma^\mu \psi_j V_\mu^- + \text{h.c}, \tag{2.9}$$

where the couplings $V_{ij}^L$ and $V_{ij}^R$ represent the left-handed and right-handed interaction strengths, respectively, between fermions and the $V^\pm$ boson. In the Standard Model, the right-handed coupling $V_{ij}^R$ is absent, reflecting the purely left-handed nature of weak interactions. The introduction of a non-zero right-handed coupling signifies new physics that allows for right-handed currents. This chiral asymmetry is responsible for the observed parity violation in weak processes and could lead to discrepancies in weak interaction measurements if the right-handed terms contribute significantly.

The Lagrangian is constructed in generic form to reflect the potential chiral asymmetry from the UV models extended SM, for instance $\mathrm{SU}(3)_c \times \mathrm{SU}(3)_L \times \mathrm{U}(1)_X$ (331) model, Left-Right Symmetric Models (LRSM), Extra-Dimensional (ED) Models, or other GUTs models, topdown ultimately. Which is a novelty we unveiled, and sets the foundation for exploring the resulting phenomenological consequences.

## 2.2 Charged scalar boson

According to the same vision and procedure as we have done with the new charged vector, the Lagrangian for a new charged scalar boson is laid out below

$$\mathcal{L}_{\mathrm{EFT}} \supset |D_\mu \phi|^2 - m_\phi^2 |\phi|^2 + \bar{\psi}_i \left( Y_{ij}^L \hat{L} + Y_{ij}^R \hat{R} \right) \psi_j \phi + \mathrm{h.c}, \tag{2.10}$$

differ from the charged vector case, information of photon interaction is completely encoded in covariant derivative $D_\mu = \partial_\mu + ieQ_\phi A_\mu$ and interacting with fermion is described by the third term. Easy to see that the coefficients in Lagrangian are valid choices, in the sense both E.O.M and energy positive definite are satisfied. In free interaction, the E.O.M

$$\partial_\mu \frac{\partial \mathcal{L}_\phi}{\partial(\partial_\mu \phi^*)} - \frac{\partial \mathcal{L}_\phi}{\partial \phi^*} = \left( \Box + m^2 \right) \phi = 0, \tag{2.11}$$

and the energy density

$$\mathcal{E} = \frac{\partial \mathcal{L}_\phi}{\partial \left( \partial_t \phi^* \right)} \left( \partial_t \phi^* \right) - \mathcal{L}_\phi = |\partial_t \phi|^2 + |\vec{\nabla} \phi|^2 + m^2 |\phi|^2 \geq 0 \tag{2.12}$$

is positive definite. In Equation 2.8, the third term highlights our focus on experimental phenomenology, paralleling our approach in the charged vector case. This investigation delves into the effects within the weak interaction regime, a domain where each chiral type manifests distinct characteristics. From the context of EFT, this allows us to offer matching constraints to constraints of several UV models, which we'll briefly touch off in Chapter **??** through the lens of the experiment. Moreover, by leveraging our computational resources, we can effectively navigate the parameter space constraints of the triplet Higgs model.

## 2.3 Feynman rule

Here we souped up an Effective Lagrangian at the low-energy scale able to be all in one expressed in the following:

$$\mathcal{L}_{\mathrm{EFT}} = \mathcal{L}_{\mathrm{SM}} + \mathcal{L}_{\mathrm{S}} + \mathcal{L}_{\mathrm{Y}} + \mathcal{L}_{\text{F-}V^{\pm}} + \mathcal{L}_{V^{\pm}} + \mathcal{L}_{\gamma}, \tag{2.13}$$

Where $\mathcal{L}_{\mathrm{SM}}$ is the well-know SM Lagrangian, and each other parts are defined

$$\mathcal{L}_{\mathrm{S}} = \left|D_\mu \phi\right|^2 - m_\phi^2 \left|\phi\right|^2, \tag{2.14}$$

$$\mathcal{L}_{\mathrm{F}} = i\bar{\psi}\ \not{D}\psi - m_f^2 \bar{\psi}\psi, \tag{2.15}$$

$$\mathcal{L}_{V^{\pm}} = -\frac{1}{2}\tilde{V}^{+}_{\mu\nu}\tilde{V}^{-\mu\nu} + m_V^2 V^{+}_{\mu} V^{-\mu} + ieQ_V a F^{\mu\nu} V^{+}_{\mu} V^{-}_{\nu}, \tag{2.16}$$

$$\mathcal{L}_{\text{F-S}} = \bar{\psi}_i \left(Y^L_{ij}\hat{L} + Y^R_{ij}\hat{R}\right)\psi_j \phi + \text{h.c}, \tag{2.17}$$

$$\mathcal{L}_{\text{F-}V^{\pm}} = \bar{\psi}_i \left(V^L_{ij}\hat{L} + V^R_{ij}\hat{R}\right)\gamma^\mu \psi_j V^{-}_{\mu} + \text{h.c} \tag{2.18}$$

according to the $U(1)_{\mathrm{EM}}$ gauge transformation

$$\partial_\mu \to D_\mu = \partial_\mu + ieQA_\mu \tag{2.19}$$

$$A_\mu \to A_\mu - \partial_\mu \alpha(x) \tag{2.20}$$

$$V^-_{\mu\nu} = \partial_\mu V^-_\nu - \partial_\nu V^-_\mu \to \tilde{V}^-_{\mu\nu} = D_\mu V^-_\nu - D_\nu V^-_\mu \tag{2.21}$$

$$\left\{\psi, \phi, V^\pm_\mu\right\} \to e^{ieQ\alpha(x)} \left\{\psi, \phi, V^\pm_\mu\right\}. \tag{2.22}$$

Be cautious, we assumed that either new charged vector or new charged scalar even though we wrote it in one line for simplification, but no interference between those. Couplings $Y^{R,L}_{ij}, V^{R,L}_{ij}$ are complex element symmetric matrices such that their left-right relative phases are $k\pi$ ($k \in \mathbb{Z}$) for CP invariant condition, and $a$ factor from an additional magnetic-moment contribution $ieQ_V aF^{\mu\nu}V^+_\mu V^-_\nu$ is purely real due to anti-symmetric of Electromagnetic Field Strength tensor $F_{\mu\nu}$. After investigating the Lepton-Flavor Violation (LFV) decay process $L \to l\gamma$ where the EFT model takes a role, we will show that only $a = 1$ for MDM/EDM renormalization. Note that, we did not include the new neutral boson here without violating any requirement from low-energy scale symmetry, while from the UV model, new charged bosons are inherently accompanied by new neutral bosons.

Moving forward, we've drawn up Feynman rules grounded in EFT Lagrangian to serve as a point of reference for our ongoing work. We'll call on the peeling method to tease out the relevant formulas from the Lagrangian. The standard procedure [3] is

1. Lower (or raise) Lorentz index of the whole fields in all way same.

2. Replace all derivatives with the $(-iq)$, in which $q$ is the incoming momenta of the fields they act on.

3. Sum up over all permutations of indices and momenta of identical external

fields.

4. Shell out all external fields from consideration.

Where step 2 acts as a means to carry out the Fourier transformation, while steps 3 and 4 are tantamount to taking the derivative of the Lagrangian vertex. The Feynman rules from the new EFT fields are then called up beneath

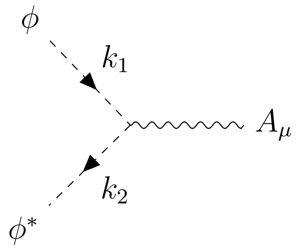


$$= -ieQ_\phi \left(k_1 + k_2\right)_\mu \tag{2.23}$$

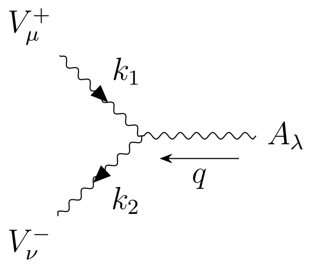


$$= -ieQ_V \left[ \left(k_2 - a.q\right)_\mu g_{\lambda\nu} + \left(k_1 + a.q\right)_\nu g_{\mu\lambda} - \left(k_1 + k_2\right)_\lambda g_{\mu\nu} \right] \tag{2.24}$$

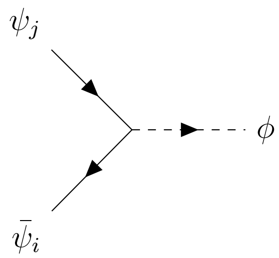


$$= i \left( Y_{ij}^L \hat{L} + Y_{ij}^R \hat{R} \right) \tag{2.25}$$

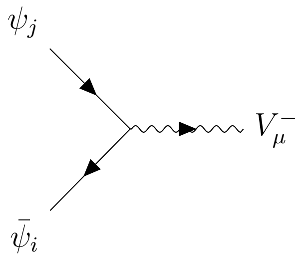


$$= i \left( V_{ij}^L \hat{L} + V_{ij}^R \hat{R} \right) \gamma_\mu \tag{2.26}$$

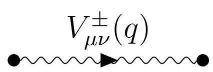


$$= \frac{-i\left(g_{\mu\nu} - \frac{q_\mu q_\nu}{m_V^2}\right)}{q^2 - m_V^2 + i\epsilon}$$

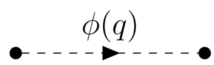


$$= \frac{i}{q^2 - m_\phi^2 + i\epsilon} \tag{2.27}$$

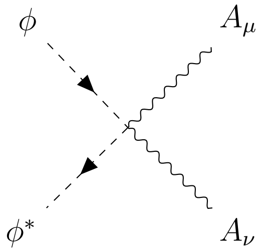


$$= 2ie^2 Q_\phi^2 g_{\mu\nu} \tag{2.28}$$

The final Feynman rule is the representative quadratic photon interaction term of scalar QED, which is not relevant to our consideration. We let Eq. 2.24 in the generic form with the free factor $\underline{a}$. In SM, it will similarly cast the rule of the $W^-$ boson as $Q_V = -1$ and $a = 1$.

# Chapter 3

# Muon decay

Muon decay was measured at TRIUMF and PSI in the '80s with polarized muons from $\pi$ decays that represent a cornerstone in the study of weak interactions, serving as a prototypical system for theoretical predictions and experimental validations in particle physics. The decay of polarized muons, in particular, offers a rich landscape for probing the underlying symmetries and mechanisms governing leptonic interactions. This investigation delves into the decay dynamics of muons within the framework of the new EFT model, exploring both the parity-nonconserving nature of weak forces and the implications of lepton universality.

The theoretical analysis herein is centered around a generalized formulation for the decay-electron distribution accommodateting polarized muon decay scenario by Michel parameters. By leveraging the polarization observables in muon decay, we aim to constrain the parameters governing weak interactions, offering insights into the validity of different theoretical constructs. This chapter is structured to initially delve into the theoretical foundation surrounding the decay parameter based on the EFT four-fermion interaction theory. This effort showcases the involvement of new physics (NP) in influencing experimental values, particularly focusing on the consequences these parameters have in polarized muon decays. Subsequently, we probe the detectable impact of NP on the Fermi constant by considering the muon lifetime.

## 3.1 Michel parameters

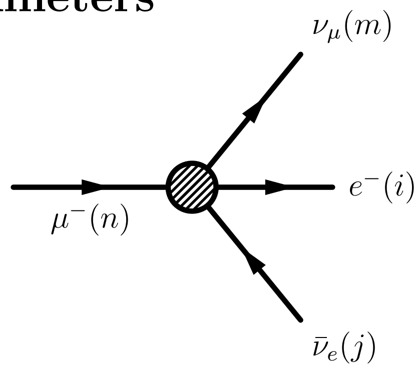


The point-like interaction in muon decay is governed by the 4-Fermi theory that is matched to the EFT couplings by the Fierz transformation. In this way, we study Michel parameters from the muon decay process to make constraints on the new couplings, and calculations in this chapter are generally able to apply to all other fermion decay modes if the massless of the final states is supposed. The differential decay rate of the muon is in the form:

$$\begin{aligned} d\Gamma = \frac{\mu^5}{3 * 2^9 * \pi^4} * (a + 4b + 6c) \Bigg\{ & 3(1-x) + 2\rho \left(\frac{4}{3}x - 1\right) \\ & -\xi \cos\theta \left[ (1-x) + 2\delta \left(\frac{4}{3} - 1\right) \right] \Bigg\} x^2 dx, \end{aligned} \tag{3.1}$$

where $\rho, \xi, \delta$ are Michel parameters [1] measured from experiment, which are defined [2]

$$\rho = \frac{3b + 6c}{a + 4b + 6c} \tag{3.2}$$

$$\delta = \frac{3b' - 6c'}{-3a' + 4b' - 14c'} \tag{3.3}$$

$$\xi = \frac{3a' - 4b' + 14c'}{a + 4b + 6c}. \tag{3.4}$$

Herein, we assumed the zero mass of outgoing particles, that caused suppression of the Michel parameter associated to the electron mass $\eta$ [4]. In Eq. 3.1, the lepton-number nonconservation is not possible to detect in muon decay, and these two parameters $\delta, \xi$ merely contribute to emitted electron distribution angle. The full treatment of the massive final state's phase space, which is useful for studying the effect of Dirac and Majorana neutrino mass in Michel parameters, is performed calculations in Appendix 8.

Note that, we consider either case, only a new scalar or new vector, where the coupling combinational parameters are defined in the new scalar case

$$a = \frac{\left|Y_{ij}^{L} Y_{nm}^{R*}\right|^2 + \left|Y_{ij}^{R} Y_{nm}^{L*}\right|^2}{16 m_\phi^4} \tag{3.5}$$

$$a' = \frac{\left|Y_{ij}^{L} Y_{nm}^{R*}\right|^2 - \left|Y_{ij}^{R} Y_{nm}^{L*}\right|^2}{16 m_\phi^4} \tag{3.6}$$

$$b = \frac{\left|Y_{ij}^{L} Y_{nm}^{L*}\right|^2 + \left|Y_{ij}^{R} Y_{nm}^{R*}\right|^2}{16 m_\phi^4} + \frac{g^4}{16 m_W^4} \tag{3.7}$$

$$b' = \frac{\left|Y_{ij}^{R} Y_{nm}^{R*}\right|^2 - \left|Y_{ij}^{L} Y_{nm}^{L*}\right|^2}{16 m_\phi^4} + \frac{g^4}{16 m_W^4} \tag{3.8}$$

$$c = \frac{\left|Y_{ij}^{L} Y_{nm}^{R*}\right|^2 + \left|Y_{ij}^{R} Y_{nm}^{L*}\right|^2}{32 m_\phi^4} \tag{3.9}$$

$$c' = \frac{\left|Y_{ij}^{R} Y_{nm}^{L*}\right|^2 - \left|Y_{ij}^{L} Y_{nm}^{R*}\right|^2}{32 m_\phi^4}, \tag{3.10}$$

or in the new vector mediator

$$a = \frac{\left|V_{ij}^{L} V_{nm}^{R*}\right|^2 + \left|V_{ij}^{R} V_{nm}^{L*}\right|^2}{m_V^4} \tag{3.11}$$

$$a' = \frac{\left|V_{ij}^{L} V_{nm}^{R*}\right|^2 - \left|V_{ij}^{R} V_{nm}^{L*}\right|^2}{m_V^4} \tag{3.12}$$

$$b = \frac{\left|V_{ij}^{L} V_{nm}^{L*}\right|^2 + \left|V_{ij}^{R} V_{nm}^{R*}\right|^2}{4 m_\phi^4} + \frac{g^4}{16 m_W^4} + \frac{g^2}{4 m_W^2 m_V^2} \mathrm{Re}\left(V_{ij}^{R} V_{nm}^{R*}\right) \tag{3.13}$$

$$b' = \frac{\left|V_{ij}^{R} V_{nm}^{R*}\right|^2 - \left|V_{ij}^{L} V_{nm}^{L*}\right|^2}{4 m_\phi^4} + \frac{g^4}{16 m_W^4} + \frac{g^2}{4 m_W^2 m_V^2} \mathrm{Re}\left(V_{ij}^{R} V_{nm}^{R*}\right) \tag{3.14}$$

are in terms of coupling parameters that we are going to constrain. Because of

$|a'| \leq a, |b'| \leq b, |c'| \leq c$, these below inequalities always hold [5]

$$|\xi\delta| \leq \rho, \tag{3.15}$$

$$0 \leq \rho \leq 1, \tag{3.16}$$

and

$$0 \leq |\xi| \leq 3 - \frac{2}{3}\rho. \tag{3.17}$$

The symmetry and anti-symmetry between left-right couplings are encoded in $\rho$ and $\delta$ respectively, particularly non-prime and prime parameters. Consequently, if only one chirality gets in that will turn out the same behavior, say, the predicted value $\rho = \delta = \frac{3}{4}$ same as Standard Model, and then constrain $|\xi| \leq 1$. The relative left-right difference effect is ascribed to $\xi$, which gives rise to changes in the angle of electron distribution. And if the true experiment turns out $|\xi| \geq 1$, it is definitely a hint of new physics involving both left-right interactions, at least in the vector boson sector or the lepton number violation interaction in Yukawa sector.

As long as the neutrinos are massless and unobserved, the scalar case is non-sensitive to LFV process on account of non-interfere between spin-0 (new scalar) and spin-1 (W boson), meanwhile this effect is charaterized by new vector case through the overlapped term.

To simplify, we further assume the universality and diagonal properties of the coupling parameters matrix, then our cases reduce to

- For scalar case

$$a = \frac{\left|Y^L\right|^2 \left|Y^R\right|^2}{8m_\phi^4} \tag{3.18}$$

$$a' = 0 \tag{3.19}$$

$$b = \frac{\left|Y^L\right|^4 + \left|Y^R\right|^4}{16m_\phi^4} + \frac{g^4}{16m_W^4} \tag{3.20}$$

$$b' = \frac{\left|Y^R\right|^4 - \left|Y^L\right|^4}{16m_\phi^4} + \frac{g^4}{16m_W^4} \tag{3.21}$$

$$c = \frac{\left|Y^L\right|^2 \left|Y^R\right|^2}{64m_\phi^4} \tag{3.22}$$

$$c' = 0. \tag{3.23}$$

- For vector case

$$a = 2\frac{\left|V^L\right|^2 \left|V^R\right|^2}{m_V^4} \tag{3.24}$$

$$a' = 0 \tag{3.25}$$

$$b = \frac{\left|V^L\right|^4 + \left|V^R\right|^4}{4m_V^4} + \frac{g^4}{16m_W^4} + \frac{g^2}{4m_W^2 m_V^2}\left|V^R\right|^2 \tag{3.26}$$

$$b' = \frac{\left|V^R\right|^4 - \left|V^L\right|^4}{4m_V^4} + \frac{g^4}{16m_W^4} + \frac{g^2}{4m_W^2 m_V^2}\left|V^R\right|^2. \tag{3.27}$$

The SM-like coupling means giving no deviation from SM contribution of Michel parameters, which are $Y^L, V^R$ will be unbounded by the Michel parameters experiment if those are in sets of SM value prediction $\rho = \delta = \frac{3}{4}, \xi = -1$. As straightforward to the eye, the universality condition implies the $\delta = \frac{3}{4}$.

## 3.2 Fermi constant

Integrating Eq. (3.1) over outgoing electron energy, the Muon decay rate is obtained

$$\Gamma = \frac{\mu^5}{3 * 2^9 * \pi^3}(a + 4b + 6c) = \frac{\mu^5 G_F^{\mu 2}}{192\pi^3}, \tag{3.28}$$

we then are able to extract the Fermi constant in terms of new coupling constants

$$(a + 4b + 6c) = 8G_F^{\mu 2}. \tag{3.29}$$

Because the lifetime of the muon is well-measured, which is thus, by far, the best determination of the Fermi constant $G_F^\mu$, and in fact, it is more than 100 times better than the other independent determination methods. In the new model scenario, the new physics positively contributes to the Fermi constant, which makes the value larger than the SM contribution. Since the new charged currents are in consideration, thus, an independent determination of the Fermi constant from the neutral current, which is in this report extracted from Z boson decay $G_F^Z$, can help to bound the allowable region of new coupling magnitudes. Furthermore, the tension between independent determinations of $G_F$, such as electroweak fits, $\mu$-decay, and CKM unitary are potentially resorted to setting a stringent NP constraint via the Standard Model EFT (SMEFT) approach [6].

- Add comment about UV model constraint in new Vector and new charge

# Chapter 4

# $L \to l\gamma$ decay process

In this chapter follow, we will delve deep into the heart of this lep-to-lep-gamma process, exploring its significance and physics implications through the lens of Feynman diagram calculations and analytical dissections. This study takes us to a deeper understanding and extracts results of Magnetic Dipole Moment (MDM) and the Lepton Flavour Violation (LFV) decay $L \to l\gamma$, then profoundly demonstrates the anomaly-free of gauge invariance of the EFT model through vanishing anapole, whose exploration is crucial for the validation of our theory. Moreover, as a progress, we will also uncover the indispensable role of extra photon coupling in contributing to the MDM of the charged vector models.

## 4.1 Gauge invariant and Anapole vanishing

Using $\mathcal{L}_{\text{EFT}}$ above to investigate the contribution to the LFV decay, that consists of all possible leading effects which only come from scalar field $\phi$ and vector field $V_\mu^\pm$ mediator. The matrix element for the process $l_j \to l_i\gamma$ emitting a real photon $\mathcal{M}^\mu = \bar{u}_i(p)\Gamma^\mu u_j(p+q)$, the interaction vertex $\Gamma^\mu$ can be formally decomposed into form factors

$$\Gamma^{\mu}(q^2=0)=\gamma^{\mu}F_1+\gamma^{\mu}\gamma_5 G_1+i\sigma^{\mu\nu}q_{\nu}F_2+i\sigma^{\mu\nu}q_{\nu}\gamma_5 G_2, \tag{4.1}$$

where $F_1, G_1$ associated to $\gamma^{\mu}$ are Dirac and Anapole form factors, gauge invariance property enforces $G_1 = 0$ though; $F_2, G_2$ associated to $\sigma^{\mu\nu}q_{\nu}$ are Magnetic Dipole (MDM) and Electric Dipole Moment (EDM) respectively. To universal interactions from the EFT Lagrangian are charged scalar $\phi$ and vector $V^{\pm}$ considered separately, where

$$F_1(G_1)=\sum_{i}^{[a,b,c,d]}F_1^{\phi,i}\left(G_1^{\phi,i}\right)+\sum_{i}^{[a,b,c,d]}F^{V,i}\left(G_1^{V,i}\right) \tag{4.2}$$

$$F_2(G_2)=\sum_{i}^{[a,b,c,d]}F_2^{\phi,i}\left(G_2^{\phi,i}\right)+\sum_{i}^{[a,b,c,d]}F^{V,2}\left(G_2^{V,i}\right) \tag{4.3}$$

we sum $\sum_i^{[a,b,c,d]}$ overall diagram contributions of each class and represent them by Passarino-Veltman (PV) convention functions [3]

$$C_{i,j,\ldots}^{V(\phi),a}=C_{i,j,\ldots}^{V(\phi),a}\left(m_2^2,0,m_1^2,m_k,m_{V(\phi)},m_{V(\phi)}\right) \tag{4.4}$$

$$C_{i,j,\ldots}^{V(\phi),d}=C_{i,j,\ldots}^{V(\phi),d}\left(m_2^2,0,m_1^2,m_{V(\phi)},m_k,m_k\right) \tag{4.5}$$

$$B_{i,j,\ldots}^{V(\phi),b}=B_{i,j,\ldots}^{V(\phi),b}\left(m_1^2,m_k,m_{V(\phi)}\right) \tag{4.6}$$

$$B_{i,j,\ldots}^{V(\phi),b}=B_{i,j,\ldots}^{V(\phi),b}\left(m_2^2,m_k,m_{V(\phi)}\right) \tag{4.7}$$

fully expressed form factors in terms of PV function are found in Appendix 8. Expanding the exact calculation of PV functions, we showed that $F_1 = G_1 = 0$, that means $\gamma^{\mu}$ terms vanish in the $l_i \to l_j + \gamma$ decay process described by generic EFT Lagrangian Eq. (2.13). Under CP transformation, the EDM $G_2$ term $\bar{\psi}\sigma_{\mu\nu}\gamma_5 F^{\mu\nu} \to -\bar{\psi}\sigma_{\mu\nu}\gamma_5 F^{\mu\nu}$ is non-invariant, which presumably are hints stemming from higher symmetry CP violation sources. As tangibly, the interaction terms in Eq. 2.13 encoded the higher symmetry model, which in general can be non-CP conserved. On the other side, the anapole term $G_1$ is not only P violated but also does not preserve gauge invariance, thus, anapole inevitably vanishes in the gauge invariant theory, otherwise the EFT theory is incomplete. In the classical regime, where the gauge invariant Lagrangian became obvious, to ascertain if there is not an anomaly in our model, checking gauge invariant in the loop level contribution is conducted, which is verified through satisfying Ward Identity

$$q_\mu \Gamma^\mu(q^2 = 0) = \not{q} F_1\left(q^2 = 0\right) + \not{q}\gamma_5 G_1\left(q^2 = 0\right) = 0 \tag{4.8}$$

with on-shell ($q^2 = 0$) photon four-momentum. In case of LFV decay, or $l_j \neq l_i$, both $F_1(q^2 = 0) = G_1(q^2 = 0) = 0$ conditions are obligated to satisfy. We are henceforth employing the assumption of a heavy charged boson $m_{V,\phi} \gg m_l$ and taking the approximated expansion at order $\mathcal{O}\left(\frac{m_l^2}{m_{V,\phi}^2}\right)$ for simplicity.

### 4.1.1 Charged vector form factors

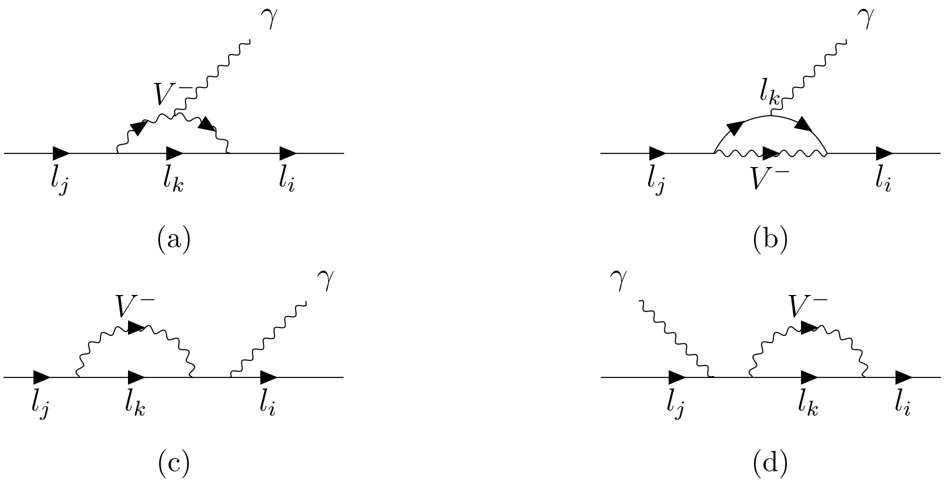


Figure 4.1: $l_j \to l_i\gamma$ with new charged vector contribution

1.

$$G_1^{V,a} = \frac{eQ_V}{24}\left\{\left(V_L^{*ki}V_L^{kj} - V_R^{*ki}V_R^{kj}\right)\left[\frac{6\left(m_j^2 - m_j m_i + m_i^2 - 3m_k^2\right)}{m_V^2}\left(\frac{1}{\epsilon} + \log\left[\frac{\mu^2}{m_V^2}\right]\right)\right.\right.$$
$$\left.\left. -18 + \frac{\left(7m_j^2 - 7m_j m_i + 7m_i^2 - 33m_k^2\right)}{m_V^2}\right] + \left(V_L^{*ki}V_R^{kj} - V_R^{*ki}V_L^{kj}\right)\frac{18\left(m_i - m_j\right)m_k}{m_V^2}\right\} \tag{4.9}$$

2.

$$G_1^{V,b} = \frac{eQ_k}{24}\left\{\left(V_L^{*ki}V_L^{kj} - V_R^{*ki}V_R^{kj}\right)\left[\frac{6\left(m_j^2 - m_j m_i + m_i^2 - 3m_k^2\right)}{m_V^2}\left(\frac{1}{\epsilon} + \log\left[\frac{\mu^2}{m_V^2}\right]\right)\right.\right.$$
$$\left.\left. -18 + \frac{\left(7m_j^2 - 7m_j m_i + 7m_i^2 - 33m_k^2\right)}{m_V^2}\right] + \left(V_L^{*ki}V_R^{kj} - V_R^{*ki}V_L^{kj}\right)\frac{18\left(m_i - m_j\right)m_k}{m_V^2}\right\} \tag{4.10}$$

3.

$$G_1^{V,c} = \frac{eQ_l}{4\left(m_i + m_j\right)}\left\{m_j\left(V_L^{*ki}V_L^{kj} - V_R^{*ki}V_R^{kj}\right)\left[\left(\frac{m_j^2 - 3m_k^2}{m_V^2}\right)\left(\frac{1}{\epsilon} + \log\left[\frac{\mu^2}{m_V^2}\right]\right) - 3\right.\right.$$
$$\left. + \frac{\left(7m_j^2 - 33m_k^2\right)}{6m_V^2}\right] + \left(Y_L^{*ki}Y_R^{kj} - Y_R^{*ki}Y_L^{kj}\right)\left[\left(6m_k + 6\frac{m_k^3}{m_V^2}\right)\left(\frac{1}{\epsilon} + \log\left[\frac{\mu^2}{m_V^2}\right]\right)\right.$$
$$\left.\left. +2m_k - \frac{m_k\left(3m_j^2 + 2m_k^2\right)}{m_V^2}\right]\right\} \tag{4.11}$$

4.

$$G_1^{V,d} = \frac{eQ_l}{4\left(m_i + m_j\right)}\left\{m_i\left(V_L^{*ki}V_L^{kj} - V_R^{*ki}V_R^{kj}\right)\left[\left(\frac{m_i^2 - 3m_k^2}{m_V^2}\right)\left(\frac{1}{\epsilon} + \log\left[\frac{\mu^2}{m_V^2}\right]\right) - 3\right.\right.$$
$$\left. + \frac{\left(7m_i^2 - 33m_k^2\right)}{6m_V^2}\right] - \left(V_L^{*ki}V_R^{kj} - V_R^{*ki}V_L^{kj}\right)\left[\left(6m_k + 6\frac{m_k^3}{m_V^2}\right)\left(\frac{1}{\epsilon} + \log\left[\frac{\mu^2}{m_V^2}\right]\right)\right.$$
$$\left.\left. +2m_k - \frac{m_k\left(3m_i^2 + 2m_k^2\right)}{m_V^2}\right]\right\} \tag{4.12}$$

The absence of the parameter $\underline{a}$ indicates that the additional interaction term involving the photon and the newly introduced charged vector does not get part in this form factor, therefore solely influencing the MDM/EDM. The pattern explicitly presents how the diagram's anapole form factor contributions are rooted out to preserve the gauged invariance. $\frac{G_1^{V,c}+G_1^{V,d}}{Q_l} = \frac{G_1^{V,b}}{Q_V} = \frac{G_1^{V,a}}{Q_k}$ corresponds to terms proportional to $\left(V_L^{*ki}Y_L^{kj} - V_R^{*ki}Y_R^{kj}\right)$ and UV finite of $\left(V_L^{*ki}V_R^{kj} - V_R^{*ki}V_L^{kj}\right)$ terms, meanwhile UV divergence in $\left(V_L^{*ki}V_R^{kj} - V_R^{*ki}V_L^{kj}\right)$ terms pertaining to $G_1^{V,c}$ and $G_1^{V,d}$ form factors canceling out each others. That manifestly combinatorial each other subtracting off even in $l_i = l_j$ case, which brings the Ward Identity $q_\mu \bar{u}_i \Lambda^\mu \left(q^2 = 0\right) u_i = \bar{u}_i \not{q} \gamma_5 G_1 \bar{u}_i = 0$ about to be obeyed. Otherwise, the Dirac form factor in the same expression within replacing $m_j \to -m_j$ and $V_L^{kj} \to -V_L^{kj}$, which however strikes divergence as $l_i = l_j$, but this divergence can be resolved through the application of the renormalization technique nonetheless.

### 4.1.2 Charged scalar form factors

In place of discussing anapole terms, we will illustrate the cancellation of the Dirac term as $m_i \neq m_j$, and the behavior of the anapole will be similarly followed.

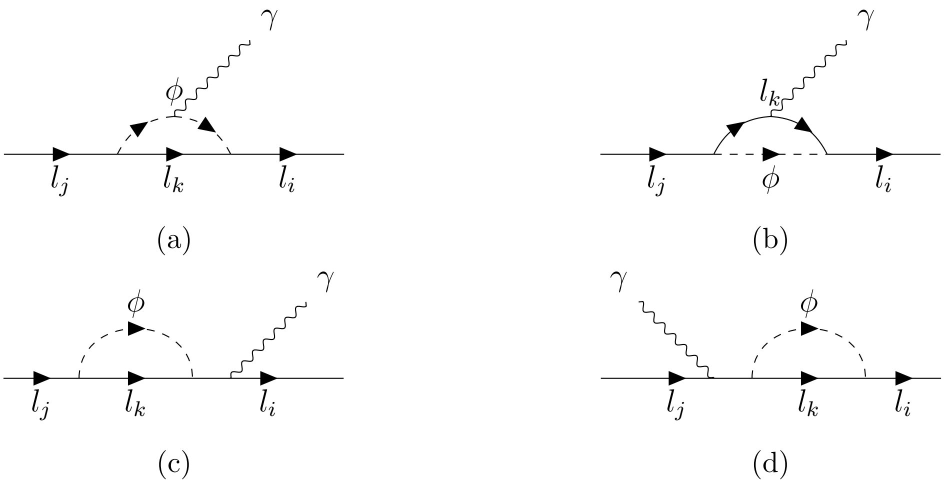


Figure 4.2: $l_j \to l_i\gamma$ with new charged scalar contribution

1.

$$
\begin{aligned}
F_1^{\phi,a} =&\frac{eQ_\phi}{8}\left\{\left(Y_L^{*ki}Y_L^{kj}+Y_R^{*ki}Y_R^{kj}\right)\left[2\left(\frac{1}{\epsilon}+\log\left[\frac{\mu^2}{m_\phi^2}\right]\right)+1\right.\right.\\
&\left.\left.+\frac{2\left(m_j^2+m_jm_i+m_i^2-3m_k^2\right)}{3m_\phi^2}\right]+2\left(Y_L^{*ki}Y_R^{kj}+Y_R^{*ki}Y_L^{kj}\right)\frac{\left(m_i+m_j\right)m_k}{m_\phi^2}\right\}
\end{aligned}
\tag{4.13}
$$

2.

$$
\begin{aligned}
F_1^{\phi,c} =&\frac{eQ_l}{8\left(m_j-m_i\right)}\left\{m_j\left(Y_L^{*ki}Y_L^{kj}+Y_R^{*ki}Y_R^{kj}\right)\left[2\left(\frac{1}{\epsilon}+\log\left[\frac{\mu^2}{m_\phi^2}\right]\right)-\frac{2\left(m_j^2-3m_k^2\right)}{3m_\phi^2}+1\right]\right.\\
&\left.+4\left(Y_L^{*ki}Y_R^{kj}+Y_R^{*ki}Y_L^{kj}\right)\left[\left(m_k-\frac{m_k^3}{m_\phi^2}\right)\left(\frac{1}{\epsilon}+\log\left[\frac{\mu^2}{m_\phi^2}\right]\right)+m_k-\frac{m_k\left(m_j^2+2m_k^2\right)}{2m_\phi^2}\right]\right\}
\end{aligned}
\tag{4.14}
$$

3.

$$
\begin{aligned}
F_1^{\phi,d} =&\frac{eQ_l}{8\left(m_i-m_j\right)}\left\{m_i\left(Y_L^{*ki}Y_L^{kj}+Y_R^{*ki}Y_R^{kj}\right)\left[2\left(\frac{1}{\epsilon}+\log\left[\frac{\mu^2}{m_\phi^2}\right]\right)-\frac{2\left(m_i^2-3m_k^2\right)}{3m_\phi^2}+1\right]\right.\\
&\left.+4\left(Y_L^{*ki}Y_R^{kj}+Y_R^{*ki}Y_L^{kj}\right)\left[\left(m_k-\frac{m_k^3}{m_\phi^2}\right)\left(\frac{1}{\epsilon}+\log\left[\frac{\mu^2}{m_\phi^2}\right]\right)+m_k-\frac{m_k\left(m_i^2+2m_k^2\right)}{2m_\phi^2}\right]\right\}
\end{aligned}
\tag{4.15}
$$

4.

$$
\begin{aligned}
F_1^{\phi,b} =&\frac{eQ_k}{8}\left\{\left(Y_L^{*ki}Y_L^{kj}+Y_R^{*ki}Y_R^{kj}\right)\left[2\left(\frac{1}{\epsilon}+\log\left[\frac{\mu^2}{m_\phi^2}\right]\right)+1\right.\right.\\
&\left.\left.+\frac{2\left(m_j^2+m_jm_i+m_i^2-3m_k^2\right)}{3m_\phi^2}\right]+2\left(Y_L^{*ki}Y_R^{kj}+Y_R^{*ki}Y_L^{kj}\right)\frac{\left(m_i+m_j\right)m_k}{m_\phi^2}\right\}
\end{aligned}
\tag{4.16}
$$

Equivalent to the charged vector case, from the above expressions, $F_1^{\phi,c}+F_1^{\phi,d} \propto F_1^{\phi,b} \propto F_1^{\phi,a}$ in such terms accompanied by $\left(Y_L^{*ki}Y_L^{kj}+Y_R^{*ki}Y_R^{kj}\right)$, respectively propositional to their own particle's charge emitting photon. They all sum up to zero if we impose $Q_l + Q_\phi + Q_k = 0$. In the $\left(Y_L^{*ki} Y_R^{kj} + Y_R^{*ki} Y_L^{kj}\right)$ terms, both $F_1^{\phi,c}$ and $F_1^{\phi,d}$ offset UV divergent parts of each other, and then the UV finite part of $F_1^{\phi}$ of altogether vanish if charge conversation is held on. The same conclusion for anapole form factors $G_1^{\phi}$ in expressions substituted $F_1^{\phi}$ by $m_j \to -m_j$ and $Y_L^{kj} \to -Y_L^{kj}$.

## 4.2 $L \to l\gamma$ and $(g-2)_l$

The ongoing dialogue between theoretical predictions and experimental measurements in the realm of the lepton $g-2$ and flavor violation decay, particularly muon, continues to be a fertile ground for discovering new physics. The measurement of the muon's anomalous magnetic moment $a_\mu$ thus remains a key focus in high-energy physics, symbolizing the intricate interplay between theoretical innovation and empirical validation.

Meanwhile, EFT models can potentially provide insights into the scale and nature of new physics that could account for the measuremental values, allowing for bridging the gap between the currently observed phenomena in the MDM/LFV measurements and the enormous of possible explanations of underlying theoretical framework, paving the way for a deeper understanding of fundamental physics. This not only aids in pinpointing the specific nature of the new interactions or particles but also helps in guiding future experimental searches.

### 4.2.1 $L \to l\gamma$ LFV decay

In the intriguing landscape of particle physics, LFV decay stands out as a phenomenon that defies the Standard Model's predictions, offering a window into potential new physics. The parity of these decays, in which a lepton of one flavor, such as a muon, transforms into another, like an electron, without conserving flavor, has fueled extensive theoretical speculation. Various models attempting to account for LFV have emerged, each proposing novel mechanisms and particles beyond the Standard Model, such as models addressing massive neutrinos, leptoquark (LQ) model, R-parity violating supersymmetry, etc. Amidst these diverse theoretical constructs, EFT plays on a bottom-up approach, which provides a versatile framework, enabling physicists to systematically analyze LFV processes without committing to a specific underlying theory smoothing the path for a deeper understanding of these rare decays.

Eq .4.1 tells us how to perform the calculation of the LFV decay rate

$$i\mathcal{M}_\nu = \bar{l}_i\left(k_i\right)\sigma^{\mu\nu}\left(F_2 + G_2\gamma_5\right)l_j\left(k_j\right)q_\mu \tag{4.17}$$

where $q = k_j - k_i$ is the on-shell emitting photon four-momentum. Assuming that the heavy mass of decaying particle $m_j \gg m_i$ we then derive the decay rate

$$\Gamma(l_j \to l_i\gamma) = \frac{m_j^3}{8\pi}\left(\left|F_2\right|^2 + \left|G_2\right|^2\right), \tag{4.18}$$

in which the squared amplitude and two-body phase space used are the following

$$|\mathbf{M}|^2 = 4m_j^4\left(\left|F_2\right|^2 + \left|G_2\right|^2\right) \tag{4.19}$$

$$\int d\mathrm{P}_2 = \int \frac{d^3k_i}{2k_i^0\left(2\pi\right)^3}\frac{d^3q}{2q^0\left(2\pi\right)^3}\left(2\pi\right)^4\delta^4\left(k_j - k_i - q\right) = \frac{\pi}{2}. \tag{4.20}$$

### 4.2.2 $(g-2)_l$ anomalous magnetics dipole moment

The measurement of the muon's anomalous magnetic moment denoted as $(g-2)$, stands as a cornerstone in precision particle physics and probes the frontiers of the Standard Model. Achieving sub-parts-per-million (ppm) precision, this measurement offers a window into physics beyond the Standard Model. The muon magnetic dipole moment, expressed as $\vec{\mu} = ge\frac{e}{2m}\vec{S}$, where $\vec{S}$ is the muon's spin angular momentum, is foundational to these explorations, Diract exactly predicted by his equation $g = 2$ in the classical limit, and then Schwinger derived $a_\mu \equiv \frac{(g-2)_\mu}{2} = \frac{\alpha}{2\pi}$ in QED first order quantum correction. Recent experimental results, particularly from the Fermilab Muon $g-2$ experiment, have corroborated earlier findings from the Brookhaven National Laboratory, intensifying the $4.2\sigma$ discrepancies between experimental data and Standard Model predictions.

On the theoretical front, efforts to reconcile these discrepancies have been robust. Theoretical physicists have proposed various extensions to the Standard Model, such as supersymmetry, leptoquarks, and dark photons, as potential explanations for the observed anomaly. These models introduce new particles or interactions that could contribute to the muon $g-2$ value, thus potentially resolving the tension between theory and experiment. Moreover, refined calculations incorporating quantum electrodynamics, hadronic contributions, and electroweak interactions have been performed, offering nuanced insights into the muon's behavior. These theoretical updates are critical for enhancing our understanding of fundamental physics, providing new directions for theoretical exploration and experimental verification.

As is customary, the EFT model proposed embarks on the game to lay on a preliminary robust stone that bridges to the higher-scale UV theories. The MDM/EDM form factor formulated in Eq. 4.1 is useful to acquire LFV decay rate

Eq. 4.18 as well, newly charged scalar and vector contribution are[1]

$$F_2^{\phi} = \frac{-e}{3.2^7 m_\phi^2 \pi^2}\Big[(m_i+m_j)(Q_\phi - 2Q_k)\left(Y_L^{*ki}Y_L^{kj} + Y_R^{*ki}Y_R^{kj}\right) + 6m_k\left(Q_\phi + 3Q_k + 2Q_k \log\left[\frac{m_k^2}{m_\phi^2}\right]\right)\left(Y_L^{*ki}Y_R^{kj} + Y_R^{*ki}Y_L^{kj}\right)\Big] \tag{4.21}$$

and

$$F_2^{V} = \frac{e}{3.2^7 m_\phi^2 \pi^2}\Big[(m_i+m_j)(Q_V - 8Q_k + 9aQ_V)\left(V_L^{*ki}V_L^{kj} + V_R^{*ki}V_R^{kj}\right) - 6m_k(5a-1)Q_V\left(V_L^{*ki}V_R^{kj} + V_R^{*ki}V_L^{kj}\right)\Big] + (a-1)\frac{eQ_V}{2^6 m_\phi^2\pi^2}\times \Big[\left(V_L^{*ki}V_L^{kj} + V_R^{*ki}V_R^{kj}\right)(m_i+m_j) - 2m_k\left(V_L^{*ki}V_R^{kj} + V_R^{*ki}V_L^{kj}\right)\Big]\left(\frac{1}{\epsilon} + \log\left[\frac{\mu^2}{m_V^2}\right]\right). \tag{4.22}$$

As mentioned earlier, the quantity $F_2^V$ exhibits UV divergence apparently popping up in Eq. 4.22 unless $a = 1$. This critical function of the extra adding-by-hand ED interaction term in the charged vector sector physicalizes $F_2^V$ to meaningful experimental prediction. Within UV theories like SM, that additional term $aieQ_V F^{\mu\nu}V_\mu^+ V_\nu^-$ naturally came out through the gauged covariant derivative approach. Nevertheless, from the EFT point of view, the matter likely springs from the missing piece of the neutral gauge boson.

The other way to cancel the divergence in the extra arbitrary magnetic moment interaction term by the $\zeta$-limiting ($\zeta \to 0$) formalism is a technical aspect of the field theory discussed by T. D. Lee and C. N. Yang [7], which introduced a negative metric deemed as ghost particle, spin-0 component in vector field with negative norm, provides a way to regulate the theory that would otherwise make the theory non-renormalizable.

[1]The MDM's form factor expressions are under the approximation of the heavily charged boson and expand to second order $\mathcal{O}\left(\frac{m_l^2}{m_{V,\phi}^2}\right)$.

Well see that, if only one chirality is involved, the charged scalar and vector contributions display negative and positive effects, respectively, on the charged ($Q_l < 0$) lepton's anomalous MDM $a_l = \frac{2m_l F_2^{V,\phi}}{-eQ_l}$ value as the $l_k$ is neutral, for instance in the SM context, or some beyond the SM contexts, like leptoquark or lepton number violation interaction structure. Conversely, the oppositely changed sign of effect would happen as the mediator is neutral ($Q_{V,\phi} = 0$) or the positively charged fermion ($Q_k > 1$) inside the loop.

The EDM form factor is achieved by switching out $m_i \to -m_i$ and $V_L^{*ki}\left(Y_L^{*ki}\right) \to -V_L^{*ki}\left(Y_L^{*ki}\right)$, roughly speaking

$$G_2^{\phi,V} \propto (m_j - m_i)\left(R^{*ki}R^{kj} - L^{*ki}L^{kj}\right) f_1 + m_k\left(R^{*ki}L^{kj} - L^{*ki}R^{kj}\right) f_2 \qquad (4.23)$$

where $L, R$ are the left and right couplings of the newly introduced charged boson and two form factors $f_1, f_2$. In $l_i = l_j$, the electric dipole value obtained from the EDM form factor is only proportional to $(R^*L^- L^*R)$. Then if the initial premise, which states that the left and right coupling's relative phase is different by an integer of pi for CP invariance (CPV-free), holds true, the EDM thus equals zero for a completely CPV-free theory.

# Chapter 5

# Constraints on (non)-Universality and non-Lepton Flavor Violation of coupling

In this chapter, we are going to discuss the constraints within the SM context, where no new charged fermion is introduced, and the non-Lepton Flavor Violation (nLFV) of the coupling scenario is equivalent to flavor diagonal coupling. We also go about investigating two universality and non-universality cases, which eventually lead to some interesting conclusions. The $Q_{V,\phi} = 1$ charged boson is the only candidate for standard model symmetries.

## 5.1 Case of universal coupling case

In this numerical analysis, we assumed the universal coupling within flavor-conserved and SM particles condition. The input parameters used are:

- $\rho = 0.74979(26)$
- $\delta = 0.75047(34)$

- $|\xi| = 1.0009^{+0.0016}_{-0.0007}$

- $G_F^{\mu} = 1.1663787(6) \times 10^{-5}$ GeV$^{-2}$

- $G_F^{Zl^+l^-} = 1.1661(16) \times 10^{-5}$ GeV$^{-2}$

- $G_F^{Z} = 1.1668(11) \times 10^{-5}$ GeV$^{-2}$

Our analysis is invalid within the $1\sigma$ uncertainty regime of Michel parameters. Thus, we hereafter extended the Michel parameters scan to $2\sigma$ and used $G_F^{Zl^+l^-}$ extracted from $\Gamma^Z_{l^+l^-} = 83.984(86)$ MeV [6, 8] and $G_F^Z$ extracted from $\Gamma_Z = 2.4952(23)$ GeV as SM inputs, then attain the plot of the scanned allowable regions below.

- For new scalar

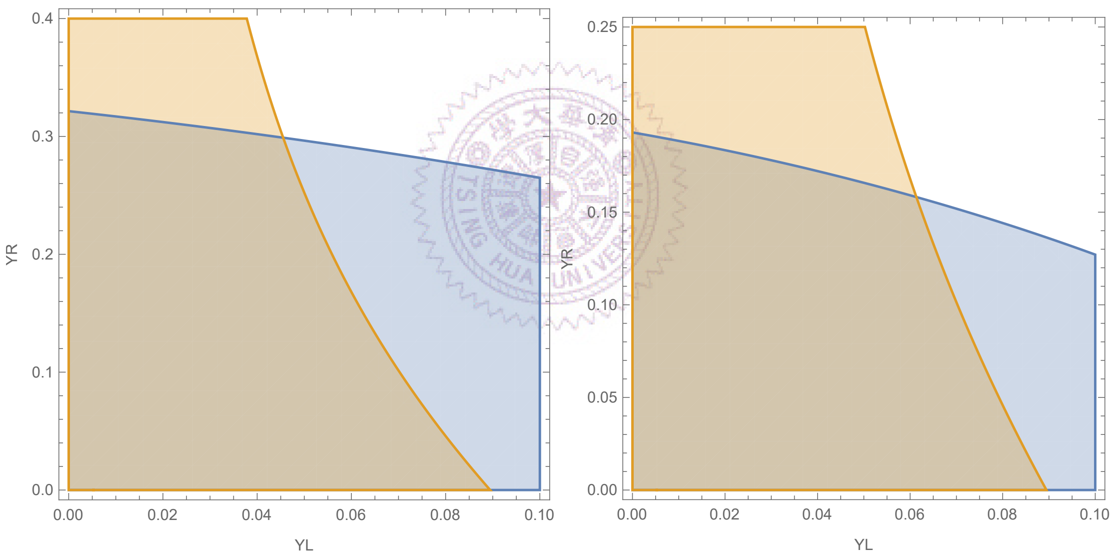


(a) $\Gamma^Z_{l^+l^-}$ input (b) $\Gamma^Z$ input

Figure 5.1: Yukawa couplings $Y$ satisfy Michel experiment values, we defined $YL \equiv \frac{|Y^L|^2/m_\phi^2}{G_F}$, $YR \equiv \frac{|Y^R|^2/m_\phi^2}{G_F}$.

- For new vector case

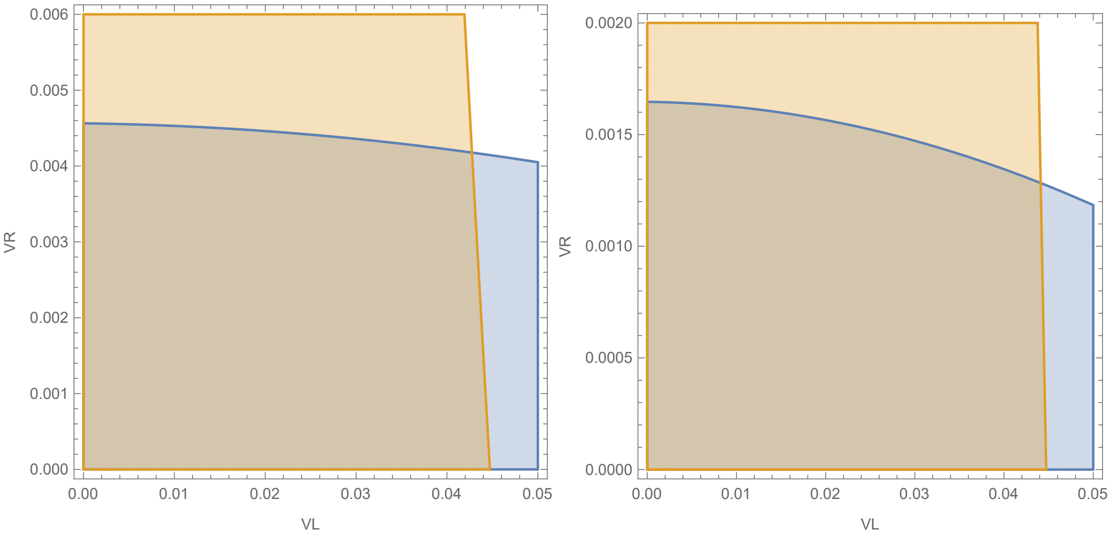


(a) $\Gamma^Z_{l^+l^-}$ input (b) $\Gamma^Z$ input

Figure 5.2: Vector couplings $V$ satisfy Michel experiment values, we defined $VL \equiv \frac{|V^L|^2/m_V^2}{G_F}$, $VR \equiv \frac{|V^R|^2/m_V^2}{G_F}$.

Where the bounded orange region is from $|\xi| = 0.9995$ constraint deviating $2\sigma$ from the mean values, whereas the bounded blue region corresponds to $G_F^{Zl^+l^-} = 1.1645 \times 10^{-5}$ or $G_F^Z = 1.1657 \times 10^{-5}$ GeV$^{-2}$ at $1\sigma$ deviation.

## 5.2 $a_l$ contributions from new charged bosons

Making use of the form factor Eq. 4.1 got calculated from Eq. [4.22,4.21] in which we derive the SM lepton's anomalous magnetic dipole

$$a_l = \frac{2m_l F_2^{V,\phi}}{e}. \tag{5.1}$$

- The contribution from Scalar field is apparently a negative effect

$$F_2^\phi = \frac{\left|Y^L\right|^2 + \left|Y^R\right|^2}{16\pi^2} \frac{m_l^4 - 2m_l^2 m_\phi^2 + \left(-2m_l^2 m_\phi^2 + 2m_\phi^4\right) \mathrm{Log}\left(\frac{m_\phi^2}{m_\phi^2 - m_l^2}\right)}{2m_l^4} \tag{5.2}$$

$$= -m_l^2 \frac{\left|Y^L\right|^2 + \left|Y^R\right|^2}{96\pi^2 m_\phi^2} + \mathcal{O}\left(\frac{m_l^3}{m_\phi^3}\right) \tag{5.3}$$

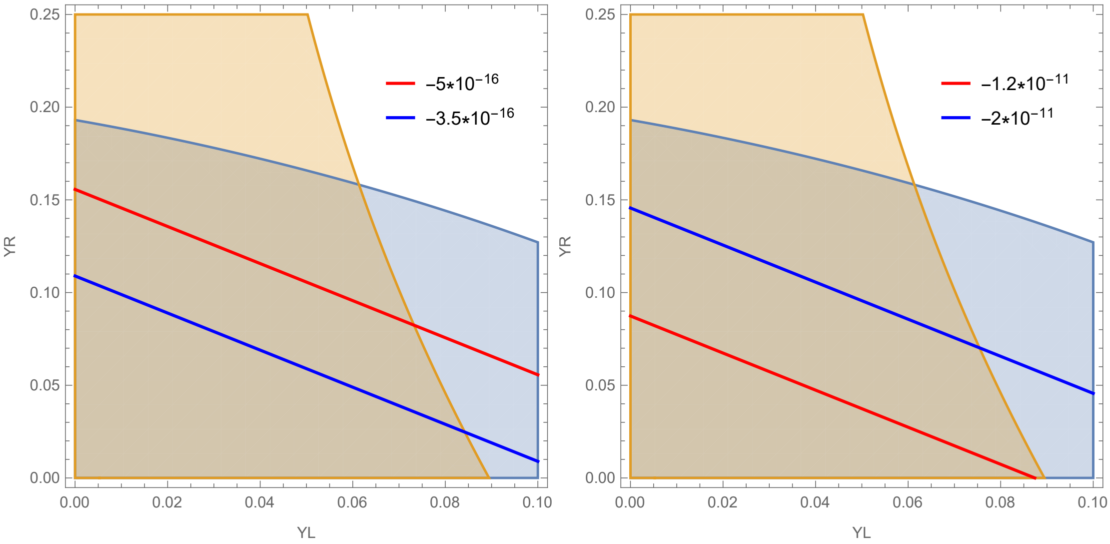


(a) Electron MDM

(b) Muon MDM

Figure 5.3: Leptonic MDM values from new scalar's constrained region

- Meanwhile, the contribution from the Vector field is positive

$$F_2^V = \frac{\left|V^L\right|^2 + \left|V^R\right|^2}{16\pi^2} \frac{m_l^6 + 8m_l^4 m_V^2 - 4m_l^2 m_V^4 + 2\left(3m_l^4 m_V^2 - 5m_l^2 m_V^4 + 2m_V^6\right) \mathrm{Log}\left(\frac{m_V^2}{m_V^2 - m_l^2}\right)}{2m_l^4 m_V^2} \tag{5.4}$$

$$= 5m_l^2 \frac{\left|V^L\right|^2 + \left|V^R\right|^2}{48\pi^2 m_V^2} + \mathcal{O}\left(\frac{m_l^3}{m_V^3}\right) \tag{5.5}$$

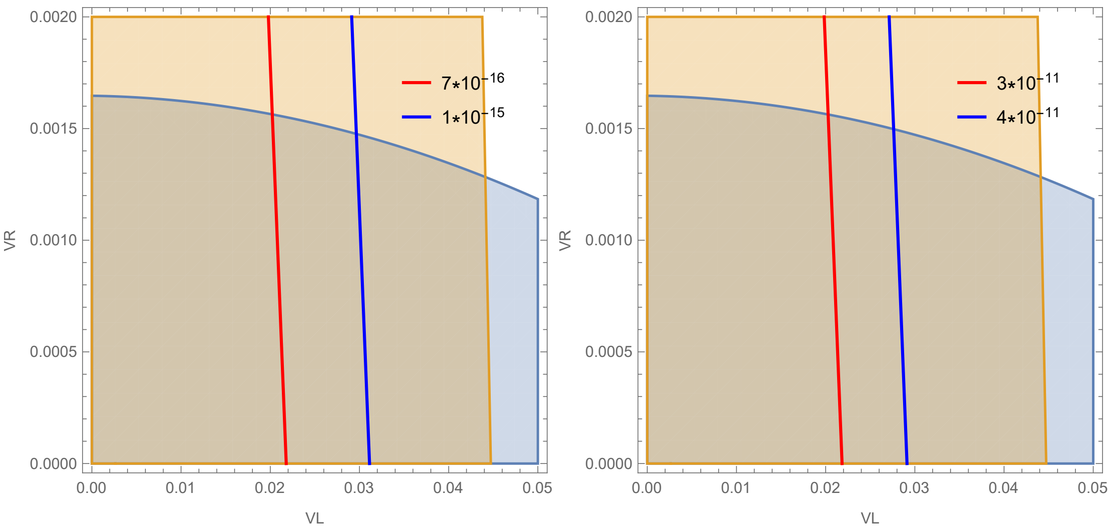


(a) Electron MDM

(b) Muon MDM

Figure 5.4: Leptonic MDM values from new Vector's constrained region

Where we used roughly the mass of new mediator $m_\phi = m_V = 10$ GeV and the constrained parameters from total Z decay. We can see that the MDM in the scalar case is highly constrained by the Fermi constant, meanwhile, the MDM is inclined to be strongly constrained by the Michel parameter $\xi$. The allowed region generates merely a smidgen of MDM values which is not enough to explain the anomaly

$$\Delta a_\mu = (2.74 \pm 0.73) \times 10^{-9} \text{ [9]} \tag{5.6}$$

$$\Delta a_e = (-88 \pm 36) \times 10^{-14} \text{ [10]}. \tag{5.7}$$

Notice that, the scalar turns out with the negative contribution and the vector with the positive contribution.

## 5.3 Case of non-universalcoupling

In the non-universality case, we thus derived the allowed region graph for explaining the electron MDM with the new scalar, hereby, we tuned the coupling of muon to a very small value $\frac{|Y^R_{\mu\nu_\mu}|^2}{m^2_\phi} = \frac{|Y^L_{\mu\nu_\mu}|^2}{m^2_\phi} = 6 \times 10^{-10}$ so as to get the safe regime in electron couplings space satisfying the electron MDM anomaly.

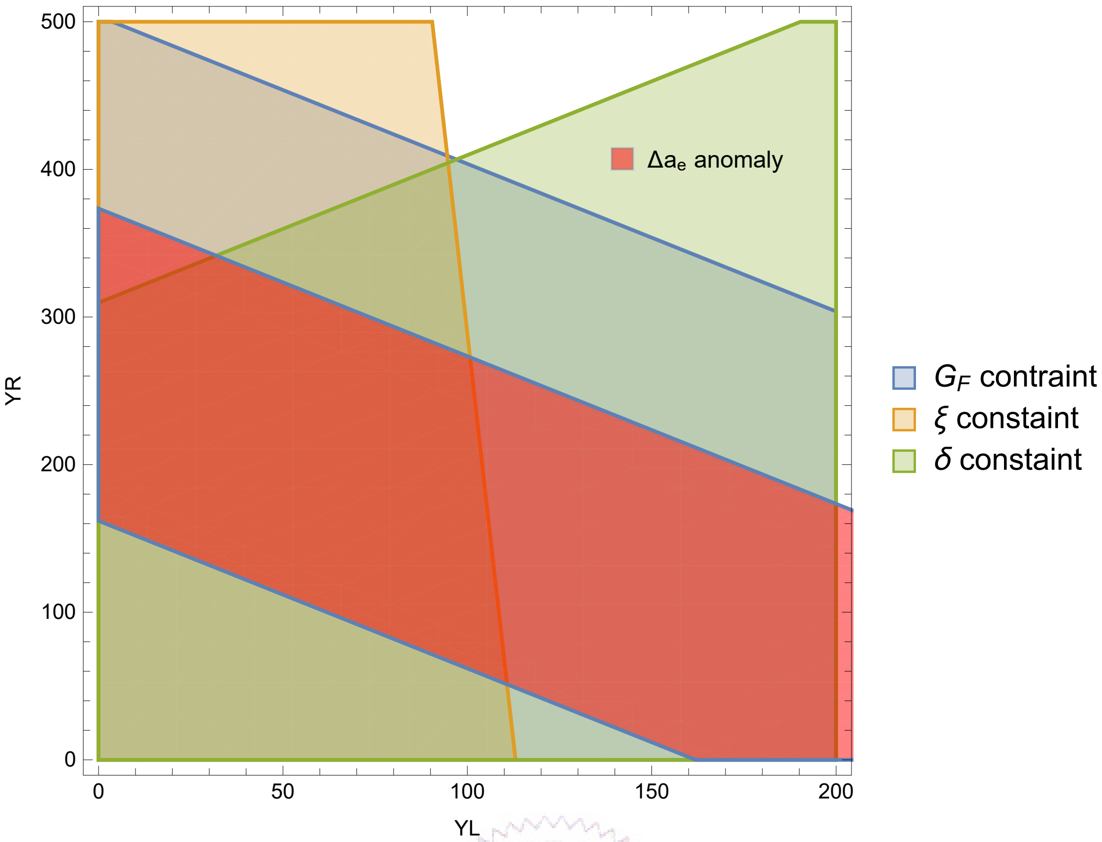


Figure 5.5: Electron MDM anomaly in the non-universality coupling new scalar's constrained region, we defined $YL \equiv \frac{|Y^L_{e\nu_e}|^2/m_\phi^2}{G_F}$, $YR \equiv \frac{|Y^R_{e\nu_e}|^2/m_\phi^2}{G_F}$.

Now, the upper bound is no longer constrained by $G_F$ as the universality case, it is instead from the Michel parameter $\delta$ constraint. Nevertheless, some complicated behavior of constraints in the non-universality new vector case, where we chose a benchmark point in the muon coupling regime that satisfies the muon MDM anomaly, and then see how the electron couplings are constrained,

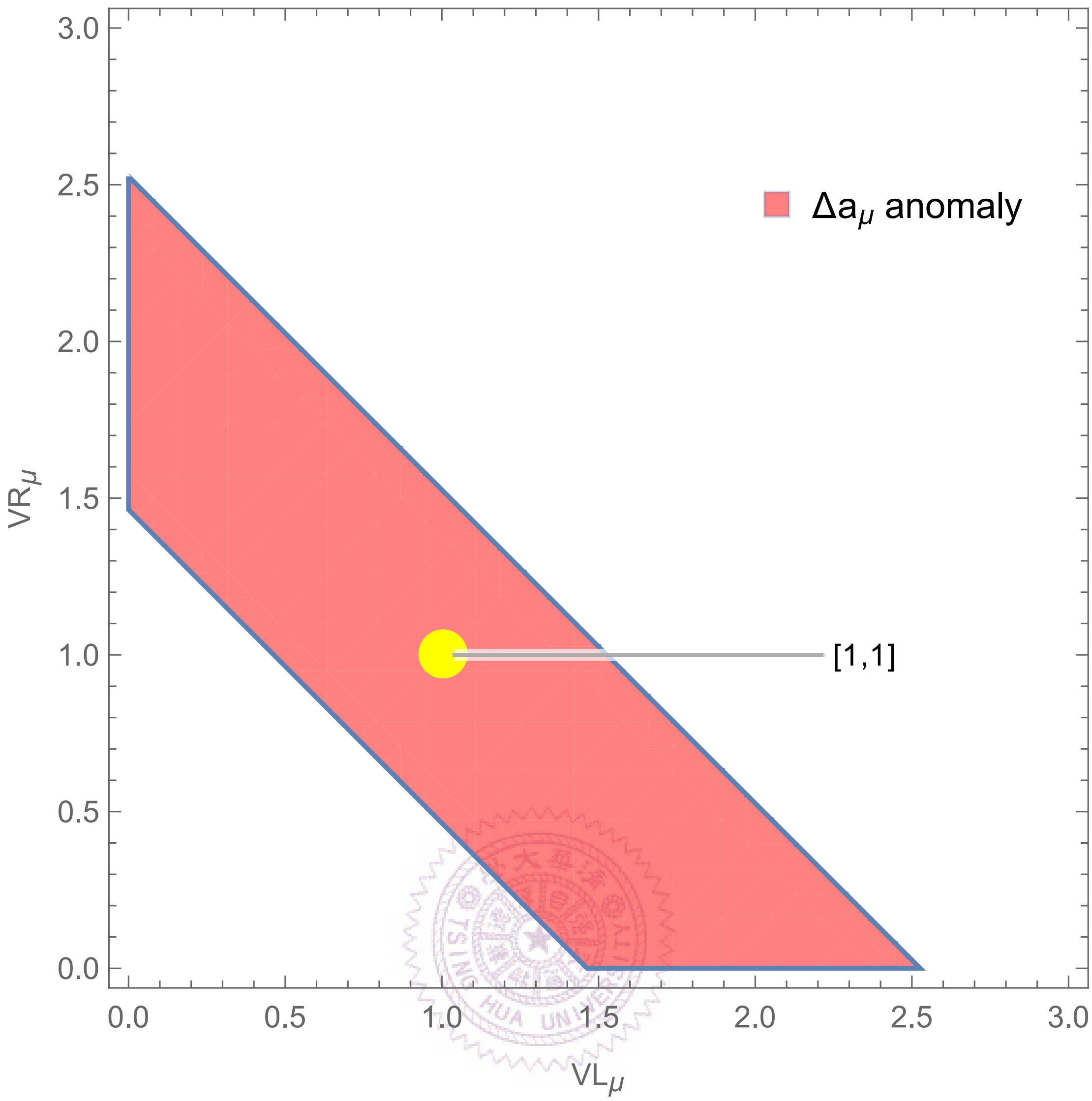


Figure 5.6: Muon MDM anomaly allowed region in the non-universality coupling new vector's case, we defined $VL_\mu \equiv \frac{|V^L_{\mu\nu_\mu}|^2/m_V^2}{G_F}$, $VR_\mu \equiv \frac{|V^R_{\mu\nu_\mu}|^2/m_V^2}{G_F}$.

Contrary to the new scalar case, the new vector has an interference effect between the new vector and the SM $W^\pm$ boson, which induces dependence on the relative phase between couplings.

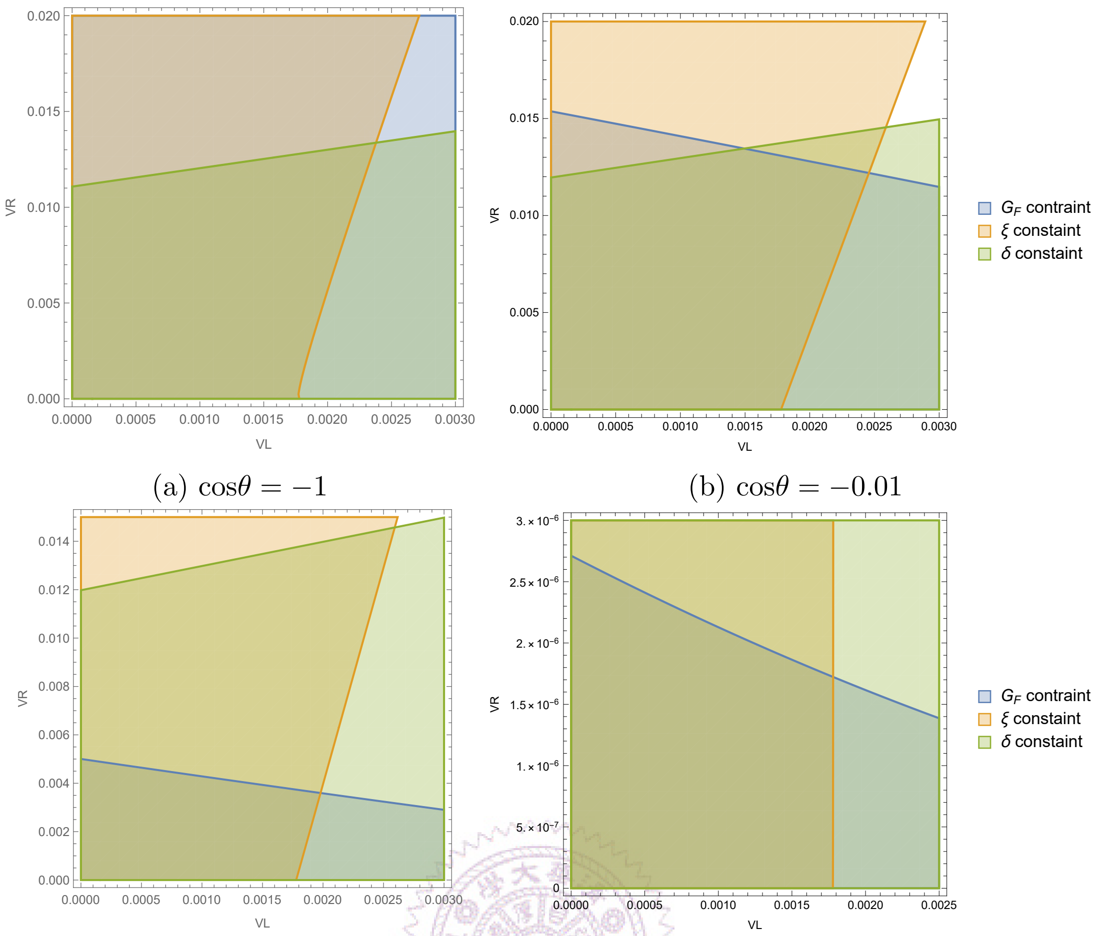


(a) $\cos\theta = -1$ (b) $\cos\theta = -0.01$

(c) $\cos\theta = 0.01$ (d) $\cos\theta = 1$

Figure 5.7: The non-universality coupling new vector's constrained region, we defined $VL \equiv \frac{|V^L_{e\nu_e}|^2/m_V^2}{G_F}$, $VR \equiv \frac{|V^R_{e\nu_e}|^2/m_V^2}{G_F}$.

The angle $\theta$ here is the relative phase between two couplings, $V^R_{e\nu_e}$ and $V^{*R}_{\mu\nu_\mu}$. As shown above in Fig. 5.7, when $\cos\theta$ is negative, the Michel parameter $\delta$ gives a strong constraint on the upper bound. Once $\cos\theta$ turns positive, the $G_F$ constraint dominates and lays down more stringent constraints in the electron coupling space.

# Chapter 6

# Constraints on Lepton Flavor Violation coupling applied to Extended Standard model Higgs sector

## 6.1 Zee's model

The Zee model, a notable extension of the Standard Model, offers a compelling framework for understanding the origin of neutrino masses, a key factor in explaining the well-established neutrino oscillation data. This model addresses the limitations of the Standard Model, particularly in explaining the tiny neutrino mass, which is realized through loop correction, apart from other mechanisms such as the type-I, II, and III seesaw models. This contribution, breaking the lepton number $L_{e,\mu,\tau}$ by two units, leads to Majorana masses for neutrinos post-electroweak symmetry breaking. It introduces new particles, including an additional Higgs doublet and a singly-charged scalar, which are not excessively heavy and thus remain within the reach of experimental verification at colliders. These new degrees of freedom are also significant in generating observable lepton flavor violating (LFV) signals, like $\mu \to e\gamma$ and $\mu \to 3e$, etc., and in potentially explaining experimental anomalies such as the anomalous MDM, baryogenesis, or even currently the CDF W boson mass anomaly. The Zee model's approach to neutrino mass generation, through one-loop Majorana neutrino masses, not only aligns with observed LFV processes but also offers testable predictions by linking these new masses and couplings to others beyond the Standard Model observables. The simplest extension of the Standard Model 2-HDM framework that entails the non-conserved lepton number interaction to give rise to the Majarona radiative neutrino mass. Thus, the leptonic Yukawa in Higgs basis is written down as:

$$\mathcal{L}_{Yuk} \supset -Y^{S}_{\alpha\beta}\overline{L^c}_{\alpha} i\sigma_2 L_\beta S^+ - Y^{H_1}_{\alpha\beta}\overline{L}_\alpha H_1 l^R_\beta - Y^{H_2}_{\alpha\beta}\overline{L}_\alpha H_2 l^R_\beta + \text{h.c.}, \tag{6.1}$$

where the first term corresponds to the singlet charged, the latter corresponds to the 2-HDM part, and the relevant Higgs potential terms are

$$V\left(H_1, H_2, S^+\right) \supset \mu H_1^{\mathrm{T}} i\sigma_2 H_2 S^- + \lambda_6 \left|H_1\right|^2 H_1^\dagger H_2 + \text{h.c.} \tag{6.2}$$

for CP-conserved in the Higgs sector, all quartic coupling is made to be real. Note that, $Y^S$ is an antisymmetric matrix and can be rephased to be real, on the other hand, $Y^{H_2}$ is generally complex, but here be considered real and leptophilic for simplicity, and the SM-like Yukawa coupling $Y^{H_1} = \frac{M_l}{<H_1>}$ in Higgs basis chosen to be diagonal without loss of generality. Briefly, the weak components

$$H_2 = \begin{pmatrix} H_2^+ \\ \frac{1}{\sqrt{2}}\left(H_2^0 + iA\right) \end{pmatrix}, \qquad H_1 = \begin{pmatrix} 0 \\ \frac{H_1^0}{\sqrt{2}} \end{pmatrix}, \qquad S^+ \tag{6.3}$$

are expressed by the mass eigenstates instead

$$\begin{pmatrix} H_{SM} \\ H_0 \end{pmatrix} = \begin{pmatrix} c_\alpha & s_\alpha \\ -s_\alpha & c_\alpha \end{pmatrix} \begin{pmatrix} H_1^0 \\ H_2^0 \end{pmatrix} \text{and} \begin{pmatrix} \eta^+ \\ H^+ \end{pmatrix} = \begin{pmatrix} c_\beta & s_\beta \\ -s_\beta & c_\beta \end{pmatrix} \begin{pmatrix} S^+ \\ H_2^+ \end{pmatrix} \tag{6.4}$$

through rotation angles. Whereas the mixing in neutral scalar induced by the Higgs potential's quartic coupling $c_\alpha s_\alpha \sim \lambda_6$ in which we consider alignment/decoupling limit ($\alpha \to 0$) being compatible with LHC search [?, ?, ?], $H_1^0 \equiv H_{SM}$ is then regarded as SM-like Higgs at 125 GeV. Though $c_\beta s_\beta = \frac{-\mu < H_1 >}{m^2_{H^+} - m^2_{\eta^+}}$ proportional to coefficient of the cubic coupling $\mu$ in Eq. (6.2) that breaks the lepton number by two units and contribute to Majorana non-zero neutrino mass matrix by quantum correction.

To clarify, we derived the relevant Feynman's rules for our calculation below

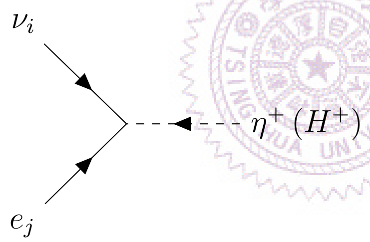


$$= -ic_\beta\,(-s_\beta)\,Y^S_{ij}\hat{L} \tag{6.5}$$

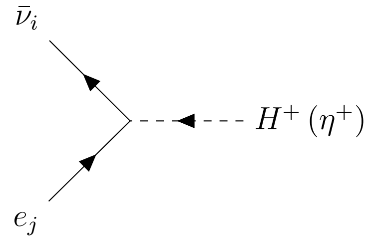


$$= -ic_\beta\,(s_\beta)\,Y^{H_2}_{ij}\hat{R} \tag{6.6}$$

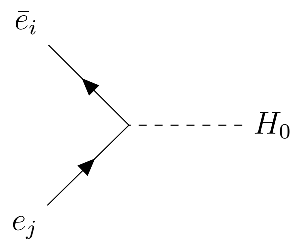


$$= -i\left(Y^{H_2}_{ij}\hat{R} + Y^{H_2 *}_{ji}\hat{L}\right) \tag{6.7}$$

### 6.1.1 Neutrino Oscillation

Neutrino oscillation, a dynamic phenomenon discovered in 1998 by the Super-Kamiokande group through their analysis of atmospheric neutrinos, stands as a pivotal exploration in elementary particle physics. Over the years, advancements in experimental studies have unveiled numerous instances of neutrino oscillation across various sources, including atmospheric, solar, accelerator, and reactor neutrinos. This groundbreaking revelation challenges the traditional understanding embedded within the Standard Model framework, proposing a new approach that necessitates the incorporation of neutrino mass and mixing into the theoretical models. As a result, neutrino oscillation emerges as a fundamental concept, promising to propel the field of particle physics toward a more comprehensive and unified understanding. The basic dynamics of the interplay between neutrino and matter is primitively written down in the charged current (CC) interaction of SM Lagrangian

$$\mathcal{L}_{\mathrm{CC}} = -\frac{g}{\sqrt{2}} W_\mu^- \sum_{l=\{e,\mu,\tau\}} \overline{\nu}_L^l \gamma^\mu l_L + \mathrm{h.c.}, \tag{6.8}$$

where the weak eigenstates $\nu_L^l$ are presented in terms of mass eigenstates $\nu_L^l = \sum_{i=1}^3 U_{li}^\nu \nu_L^i$ by an $3 \times 3$ unitary mixing matrix $U^\nu$, the so-called Pontecorvo-Maki-Nakagawa-Sakata (PMNS) matrix which is characterized by the following standard parametrization

$$U^\nu = \begin{pmatrix} 1 & 0 & 0 \\ 0 & c_{23} & s_{23} \\ 0 & -s_{23} & c_{23} \end{pmatrix} \times \begin{pmatrix} c_{13} & 0 & s_{13}e^{-i\delta_{CP}^D} \\ 0 & 1 & 0 \\ -s_{13}e^{i\delta_{CP}^D} & 0 & c_{13} \end{pmatrix} \times \begin{pmatrix} c_{12} & s_{12} & 0 \\ -s_{12} & c_{12} & 0 \\ 0 & 0 & 1 \end{pmatrix} \times \mathrm{Diag}\left(1, e^{i\frac{\mu_1}{2}}, e^{i\frac{\mu_2}{2}}\right)$$
$$= \begin{pmatrix} c_{12}c_{13} & s_{12}c_{13} & s_{13}e^{-i\delta_{CP}^D} \\ -s_{12}c_{23} - c_{12}s_{23}s_{13}e^{i\delta_{CP}^D} & c_{12}c_{23} - s_{12}s_{23}s_{13}e^{i\delta_{CP}^D} & s_{23}c_{13} \\ s_{12}s_{23} - c_{12}c_{23}s_{13}e^{i\delta_{CP}^D} & -c_{12}s_{23} - s_{12}c_{23}s_{13}e^{i\delta_{CP}^D} & c_{23}c_{13} \end{pmatrix} \times \mathrm{Diag}\left(1, e^{i\frac{\mu_1}{2}}, e^{i\frac{\mu_2}{2}}\right) \tag{6.9}$$

in terms of mixing angles $c_{ij}\,(s_{ij})$ and CP phases $\{\mu_i, \delta_{CP}^D\}$. In SM formalism, the neutrino is massless, or the PMNS matrix is the identity matrix in other words. The neutrino oscillation detected in 1998 was an obvious evidence of BSM new physics that forced us to discriminate between the weak eigenstate and mass eigenstate of neutrino, which is generated through the interaction with the W boson and Higgs boson respectively. The mass eigenstate is usually regarded as the physical state due to the invariance under Lorentz transformation, with a definite mass generated in the Yukawa sector.

- Dynamics and the mixing angle, like decay processes related to detecting mixing angles
- counting d.o.f. in PMNS matrix
- Dirac and Majarona mass Lagrangian
- Review all types of model generating neutrnino mass
- Zee model

particularly one-loop order in this study's context

$$M_\nu = \frac{s_\beta c_\beta}{8\pi^2} \log\left(\frac{m_{\eta^+}^2}{m_{H^+}^2}\right) \left[Y^S M_l \left(Y^{H_2}\right)^{\mathrm{T}} + Y^{H_2} M_l \left(Y^S\right)^{\mathrm{T}}\right]. \tag{6.10}$$

### 6.1.2 Trilepton decay constraint

The only contribution to LFV trilepton decay $l_i- \to l_j \bar{l}_m l_n$ comes from the new neutral $H_0$ scalar, which we can traverse all $Y^{H_2}$ coupling contraints

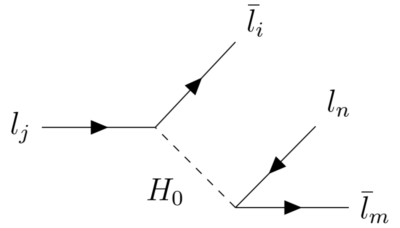


$$\to \Gamma\left(l_i \to l_j \bar{l}_m l_n\right) = \frac{m_i^5 \mathbf{Y}}{n!3.2^9\pi^3}. \tag{6.11}$$

The decay rate is derived in the approximation $m_j, m_n, m_m \ll m_i$, which we can ignore the final state masses, and the factor $\mathbf{Y}$ holds in the information of Yukawa coupling of the second Higgs doublet

$$\begin{aligned}\mathbf{Y} =& \frac{1}{16m_{H_0}^4}\Big(\left|2Y_{ji}^{H_2}Y_{nm}^{H_2*} - Y_{mi}^{H_2}Y_{nj}^{H_2*}\right|^2 + \left|2Y_{ij}^{H_2}Y_{mn}^{H_2*} - Y_{im}^{H_2}Y_{jn}^{H_2*}\right|^2 + 4\left|Y_{ji}^{H_2}Y_{mn}^{H_2}\right|^2 \\ &+4\left|Y_{ij}^{H_2}Y_{nm}^{H_2}\right|^2 + 3\left|Y_{mi}^{H_2}Y_{nj}^{H_2}\right|^2 + 3\left|Y_{im}^{H_2}Y_{jn}^{H_2}\right|^2 + 4\left|Y_{mi}^{H_2}Y_{jn}^{H_2}\right|^2 + 4\left|Y_{im}^{H_2}Y_{nj}^{H_2}\right|^2\Big).\end{aligned} \tag{6.12}$$

Employing the branching ratio

$$Br\left(l_i \to l_j \bar{l}_m l_n\right) = \frac{\mathbf{Y}}{n!128G_F^{i2}} Br\left(l_i \to l_j \bar{\nu}_m \nu_n\right), \tag{6.13}$$

where $G_F^i$ is the Fermi constant determined in the lepton $l_i$ decay rate process and $n!$ counts for undistinguished outgoing particles, we plugin the experiment data to set out the upper-bound constraint table 6.1 below

| Process | Exp. data | Coupling | Constraint $\left(\frac{m_{H_0}}{GeV}\right)^4$ |
|---|---|---|---|
| $\mu^- \to e^- e^+ e^-$ | $< 10^{-12}$ | $\left\|Y_{ee}^{H_2}\right\|^2 \left(\left\|Y_{e\mu}^{H_2}\right\|^2 + \left\|Y_{\mu e}^{H_2}\right\|^2\right)$ | $< 2.9 \times 10^{-21}$ |
| $\tau^- \to e^- e^+ e^-$ | $< 2.7 \times 10^{-8}$ | $\left\|Y_{ee}^{H_2}\right\|^2 \left(\left\|Y_{e\tau}^{H_2}\right\|^2 + \left\|Y_{\tau e}^{H_2}\right\|^2\right)$ | $< 4.47 \times 10^{-16}$ |
| $\tau^- \to \mu^- \mu^+ \mu^-$ | $< 2.1 \times 10^{-8}$ | $\left\|Y_{\mu\mu}^{H_2}\right\|^2 \left(\left\|Y_{\tau\mu}^{H_2}\right\|^2 + \left\|Y_{\mu\tau}^{H_2}\right\|^2\right)$ | $< 3.48 \times 10^{-16}$ |
| $\tau^- \to e^- \mu^+ e^-$ | $< 1.5 \times 10^{-8}$ | $\left\|Y_{\mu e}^{H_2}\right\|^2 \left\|Y_{e\tau}^{H_2}\right\|^2 + 2\left\|Y_{e\mu}^{H_2}\right\|^2 \left\|Y_{e\tau}^{H_2}\right\|^2$ $+\left\|Y_{e\mu}^{H_2}\right\|^2 \left\|Y_{\tau e}^{H_2}\right\|^2 + 2\left\|Y_{\mu e}^{H_2}\right\|^2 \left\|Y_{\tau e}^{H_2}\right\|^2$ | $< 7.45 \times 10^{-16}$ |
| $\tau^- \to \mu^- e^+ \mu^-$ | $< 1.7 \times 10^{-8}$ | $\left\|Y_{e\mu}^{H_2}\right\|^2 \left\|Y_{\mu\tau}^{H_2}\right\|^2 + 2\left\|Y_{e\mu}^{H_2}\right\|^2 \left\|Y_{\tau\mu}^{H_2}\right\|^2$ $+\left\|Y_{\mu e}^{H_2}\right\|^2 \left\|Y_{\tau\mu}^{H_2}\right\|^2 + 2\left\|Y_{\mu e}^{H_2}\right\|^2 \left\|Y_{\mu\tau}^{H_2}\right\|^2$ | $< 8.45 \times 10^{-16}$ |
| $\tau^- \to \mu^- \mu^+ e^-$ | $< 2.7 \times 10^{-8}$ | $\left\|2Y_{\mu\tau}^{H_2} Y_{\mu e}^{H_2 *} - Y_{e\tau}^{H_2} Y_{\mu\mu}^{H_2 *}\right\| + 4\left\|Y_{\mu\tau}^{H_2}\right\|^2 \left\|Y_{e\mu}^{H_2}\right\|^2$ $+\left\|2Y_{\tau\mu}^{H_2 *} Y_{e\mu}^{H_2} - Y_{\tau e}^{H_2 *} Y_{\mu\mu}^{H_2}\right\| + 4\left\|Y_{\tau\mu}^{H_2}\right\|^2 \left\|Y_{\mu e}^{H_2}\right\|^2$ $+7\left\|Y_{e\tau}^{H_2}\right\|^2 \left\|Y_{\mu\mu}^{H_2}\right\|^2 + 7\left\|Y_{\tau e}^{H_2}\right\|^2 \left\|Y_{\mu\mu}^{H_2}\right\|^2$ | $< 2.69 \times 10^{-15}$ |
| $\tau^- \to e^+ \mu^- e^-$ | $< 1.8 \times 10^{-8}$ | $\left\|2Y_{e\tau}^{H_2} Y_{e\mu}^{H_2 *} - Y_{\mu\tau}^{H_2} Y_{ee}^{H_2 *}\right\| + 4\left\|Y_{e\tau}^{H_2}\right\|^2 \left\|Y_{\mu e}^{H_2}\right\|^2$ $+\left\|2Y_{\tau e}^{H_2 *} Y_{\mu e}^{H_2} - Y_{\tau\mu}^{H_2 *} Y_{ee}^{H_2}\right\| + 4\left\|Y_{\tau e}^{H_2}\right\|^2 \left\|Y_{e\mu}^{H_2}\right\|^2$ $+7\left\|Y_{\mu\tau}^{H_2}\right\|^2 \left\|Y_{ee}^{H_2}\right\|^2 + 7\left\|Y_{\tau\mu}^{H_2}\right\|^2 \left\|Y_{ee}^{H_2}\right\|^2$ | $< 1.79 \times 10^{-15}$ |

Table 6.1: Trilepton decay constraints table

the well-know values of lepton decay branching ratio $Br\left(\mu \to e\bar{\nu}_e\nu_\mu\right) \approx 100\%$ and $Br\left(\tau \to l\bar{\nu}_l\nu_\tau\right) \approx 17.5\%$ are used here. These constraints roughly tell us the upper bound of the new doublet Higg coupling $\left|Y^{H_2}\right| < \mathcal{O}\left(10^{-4}\right)\frac{m_{H_0}}{GeV}$.

### 6.1.3 Muon decay

In the compass of this study, the only come-up from singlet scalar solely strikes up from lepton decay which interferes with contributions of doublet charged Higgs. The Feynman diagrams scale up from 2 to 8 after mass diagonalization, inducing the singlet-doublet interference terms. The first two contributions from singlet and doublet respectively

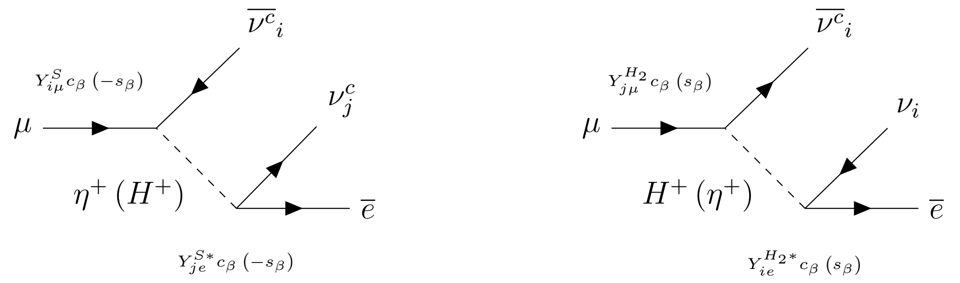

$(a)$ $(b)$

The two Michel parameters keep intact $\rho = \delta = \frac{3}{4}$ compared to SM prediction despite these two unmixed effects from singlet and doublet charged scalar above get into, which is due to their non-sensitivity to the chirality distinction. Meanwhile, the $\xi$ parameter is able to achieve the new physics effect through $b(b')$ parameter as defined in Eq (**??**)

$$b\,(b') = \left(\sqrt{2} G_F^{SM} + \frac{\left|Y^S_{e\mu}\right|^2}{4 m_S^2}\right)^2 + \frac{1}{16 m_S^4} \sum_{i,j \neq \{e,\mu\}} \left|Y^S_{i\mu}\right|^2 \left|Y^S_{je}\right|^2 + (-) \frac{1}{16 m^4_{H_2^+}} \sum_{i,j} \left|Y^{H_2}_{i\mu}\right|^2 \left|Y^{H_2}_{je}\right|^2, \tag{6.14}$$

where $m_S$, $m_{H_2^+}$ are the mass of singlet and doublet respectively, after mass diagonalization, we substitute

$$\frac{1}{m_S^2} \to \frac{c_\beta^2}{m^2_{\eta^+}} + \frac{s_\beta^2}{m^2_{H^+}} \tag{6.15}$$

$$\frac{1}{m^2_{H_2^+}} \to \frac{s_\beta^2}{m^2_{\eta^+}} + \frac{c_\beta^2}{m^2_{H^+}} \tag{6.16}$$

to get the physical result. The aforementioned intrinsic difference between chiral scalar and vector-form couplings brought up the sign change of $b$ relative to $b'$. Notably, as mentioned in Chapter 3, the scalar coupling from the doublet has no intertwining with respect to vector-form coupling attributed to the spin-flip difference, that produces the $\xi$ constraint as a corollary. In contrast, the first diagram with Lepton Number Violation (LNV) Yukawa couplings puts on the vector-like form after Fierz transformation, for instance

$$\begin{aligned}
\overline{\nu^c}_e \hat{L}\mu \; \overline{e}\hat{R}\nu_\mu^C \;\; &\xrightarrow[\text{Transform}]{\text{Fierz}} \;\; -\frac{1}{4}\left[\overline{\nu}_\mu\gamma^\mu\nu_e \; \overline{e}_L\gamma_\mu\mu_L + \overline{\nu}_\mu\gamma^\mu\gamma_5\nu_e \; \overline{e}_L\gamma_\mu\gamma_5\mu_L\right] \\
&\xrightarrow[\text{Transform}]{\text{Fierz}} \; \frac{1}{2} \; \overline{e}\gamma^\mu\hat{L}\nu_e \; \overline{\nu}_\mu\gamma_\mu\hat{L}\mu,
\end{aligned} \tag{6.17}$$

therefore exhibiting a strong interference with W boson, the new effect thereof just only shows up in Fermi constant constraint, where we will pick up that later.

The next four diagrams present the mixing properties between normal and LNV Yukawa couplings that open the possibility of detecting new physics in Michel parameters

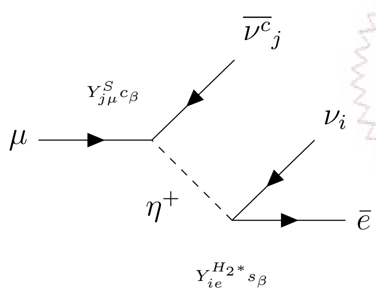


$(c)$

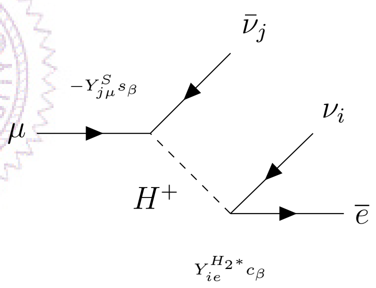


$(d)$

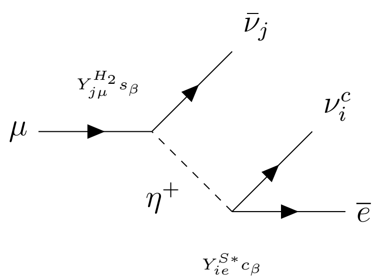


$(e)$

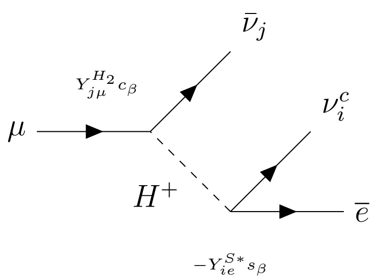


$(f)$

These two distinct processes display the lepton number violation $\triangle L = -2$ for the first two diagrams and $\triangle L = 2$ for the latter two. The interference effect between singlet and doublet scalar gives rise to non-trivial contribution to decay parameters, which interestingly displays pseudo-left-right mixing effect by through the coupling combinational parameters Eq. (3.6-3.10)

$$a_{-2} = a'_{-2} = \left(\frac{1}{m^2_{\eta^+}} - \frac{1}{m^2_{H^+}}\right)^2 \frac{c^2_\beta s^2_\beta}{16} \left| Y^S_{j\mu} Y^{H_2 *}_{ie} - Y^S_{i\mu} Y^{H_2 *}_{je} \right|^2 \tag{6.18}$$

$$c_{-2} = -c'_{-2} = \left(\frac{1}{m^2_{\eta^+}} - \frac{1}{m^2_{H^+}}\right)^2 \frac{c^2_\beta s^2_\beta}{16} \left| Y^S_{j\mu} Y^{H_2 *}_{ie} + Y^S_{i\mu} Y^{H_2 *}_{je} \right|^2 \tag{6.19}$$

and

$$a_2 = -a'_2 = \left(\frac{1}{m^2_{\eta^+}} - \frac{1}{m^2_{H^+}}\right)^2 \frac{c^2_\beta s^2_\beta}{16} \left| Y^{H_2}_{j\mu} Y^{S*}_{ie} - Y^{H_2}_{i\mu} Y^{S*}_{je} \right|^2 \tag{6.20}$$

$$c_2 = c'_2 = \left(\frac{1}{m^2_{\eta^+}} - \frac{1}{m^2_{H^+}}\right)^2 \frac{c^2_\beta s^2_\beta}{16} \left| Y^{H_2}_{j\mu} Y^{S*}_{ie} + Y^{H_2}_{i\mu} Y^{S*}_{je} \right|^2 \tag{6.21}$$

corresponding to $\triangle L = -2$, $\triangle L = 2$ respectively, with no effect on $b$, $b'$ at all. Consequently, the total contribution to parameters $a(a') = a(a')_2 + a(a')_{-2}$ and $c(c') = c(c')_2 + c(c')_{-2}$ alters the two Michel parameters $\rho$, $\delta$ from their SM values

$$\triangle\rho = \frac{3}{16}\left(\frac{1}{m^2_{\eta^+}} - \frac{1}{m^2_{H^+}}\right)^2 \frac{c^2_\beta s^2_\beta}{a+4b+6c} \mathrm{Re}\left(Y^{H_2}_{j\mu} Y^{S*}_{ie} Y^{H_2 *}_{i\mu} Y^S_{je} + Y^S_{j\mu} Y^{H_2 *}_{ie} Y^{S*}_{i\mu} Y^{H_2}_{je}\right)$$
$$= (-47 - 5) \times 10^{-5} \tag{6.22}$$

$$\triangle\delta = \frac{21}{16}\left(\frac{1}{m^2_{\eta^+}} - \frac{1}{m^2_{H^+}}\right)^2 \frac{c^2_\beta s^2_\beta}{-3a'+4b'-14c'} \mathrm{Re}\left(Y^{H_2}_{j\mu} Y^{S*}_{ie} Y^{H_2 *}_{i\mu} Y^S_{je} - Y^S_{j\mu} Y^{H_2 *}_{ie} Y^{S*}_{i\mu} Y^{H_2}_{je}\right)$$
$$= (1.3 - 8.1) \times 10^{-4}. \tag{6.23}$$

Finally, all new physics effects in muon decay are boiled down in $\xi$ constraint

$$|\triangle\xi| = \frac{1}{2}\left(\frac{1}{m^2_{\eta^+}} - \frac{1}{m^2_{H^+}}\right)^2 \frac{c^2_\beta s^2_\beta}{a+4b+6c} \mathrm{Re}\left(\frac{3}{2} Y^{H_2}_{j\mu} Y^{S*}_{ie} Y^{H_2 *}_{i\mu} Y^S_{je} - Y^S_{j\mu} Y^{H_2 *}_{ie} Y^{S*}_{i\mu} Y^{H_2}_{je}\right)$$
$$+ \frac{1}{2}\left(\frac{1}{m^2_{\eta^+}} - \frac{1}{m^2_{H^+}}\right)^2 \frac{c^2_\beta s^2_\beta}{a+4b+6c}\left(\left|Y^{H_2}_{j\mu}\right|^2 \left|Y^S_{ie}\right|^2 + \left|Y^{H_2}_{i\mu}\right|^2 \left|Y^S_{je}\right|^2\right) + \frac{1}{8 m^4_{H_2^+}} \sum_{i,j} \frac{\left|Y^{H_2}_{i\mu}\right|^2 \left|Y^{H_2}_{je}\right|^2}{a+4b+6c}$$
$$= (2 - 25) \times 10^{-4}, \tag{6.24}$$

and Fermi constant. As mentioned earlier, the Fermi constant is often deemed as an anomaly source of new physics contribution, in which the Zee model contributions play the new physics role, and as in the previous usage in Chapter **??**, Z boson decay is benchmarked for Standard Model contribution $G_F^{SM} \equiv G_F^Z$ compared to Fermi constant $G_F^\mu$ precisely measured in muon decay Eq. (3.29)

$$\begin{aligned}
\triangle G_F^2 &= \left(G_F^{\mu 2}\right)^2 - \left(G_F^{SM}\right)^2 = \frac{a+4b+6c}{8} - \left(G_F^{SM}\right)^2 \\
&= \frac{G_F^{SM}}{2\sqrt{2}m_S^2}\left|Y_{e\mu}^S\right|^2 + \frac{1}{32m_S^4}\sum_{i,j}\left|Y_{i\mu}^S\right|^2\left|Y_{je}^S\right|^2 \\
&+ \frac{1}{32m_{H_2^+}^4}\sum_{i,j}\left|Y_{i\mu}^{H_2}\right|^2\left|Y_{je}^{H_2}\right|^2 + \frac{a+6c}{8}.
\end{aligned} \tag{6.25}$$

The first three terms are caused by purely singlet and doublet effects Eq. (6.14), meanwhile the last term comes from singlet-doublet mixing effect Eq. (6.18-6.21). Roughly speaking, from the above expression of Fermi constant constraint, where $\triangle G_F^2 \sim \mathcal{O}\left(10^{-13}\right)$ GeV$^2$, the coupling strength $\frac{\left|Y^{S,H_2}\right|^2}{m^2_{S,H_2^+}} < \mathcal{O}\left(10^{-6}\right)$ GeV$^{-2}$ cannot be too large. Along with Eq. (6.23) of the Michel parameter $\delta$, roughly estimating $\frac{\left|Y^{S,H_2}\right|^2}{m^2_{S,H_2^+}} > \frac{\mathcal{O}\left(10^{-7}\right)}{c_\beta s_\beta}$ GeV$^{-2}$, where $-3a' + 4b' - 14c' \sim G_F^2 \sim \mathcal{O}\left(10^{-10}\right)$ GeV$^2$ and $c_\beta s_\beta = \frac{-\mu < H_1 >}{m^2_{H^+} - m^2_{\eta^+}}$. Therefore, the cubic coupling $\mu$ in Eq. (6.2) is forbidden to be arbitrarily small, and the lower bound first-step estimation is inferred

$$\mu > m^2_{\eta^+, H^+} \times \mathcal{O}\left(10^{-3}\right) \text{GeV}, \tag{6.26}$$

or in particular case of the much heavier one in $\mathcal{O}\left(1\right)$ TeV scale mass range induces $\mu > \mathcal{O}\left(10^3\right)$ GeV.

## 6.2 Triplet Higgs Model

The reason we are interested in this modern is because it introduced the correlation between rare decay processes within enough free parameters to reconcile neutrino mass issues. In this scope of the thesis, we neglect tiny value $\frac{\mu}{m_\triangle} \approx 0$ which causes negligibly mixing in the Higgs sector and triplet VEV, so that we can mainly focus on the effects of the new triplet's Yukawa sector with approximation mass of all triplet scalars $\approx m_\triangle$. The Yukawa sector encoded new triplet's contributions to our concerned process is presented in Lagrangian term

$$\mathcal{L}_{Yuk} \supset -Y^{\triangle}_{\alpha\beta}\overline{L^c}_{\alpha}\tilde{\triangle} L_\beta + \text{h.c.}, \tag{6.27}$$

where $\tilde{\triangle} = i\sigma_2\triangle$ is a triplet scalar transforming under adjoint representation of $\mathrm{SU}(2)_L$ group.

# Chapter 7

# Conclusion and Outlook

In conclusion, this study's establishment of the low-energy EFT incorporating a novel charged boson at a low-energy scale aims to mark a significant insight into our understanding of the weak sector. The thorough verification of the anapole moment's vanishing at the one-loop order within this framework not only solidifies the theoretical footing of our approach but also assures the theoretically allowable contributions we should take into account. In addition, the extra electromagnetic interaction of the charged vector is requisite to MDM renormalized contribution, this intriguing component may hint at a novel physics originating from a neutral vector boson.

Our investigations into the lens of leptonic decays, have enabled us to place stringent constraints on the newly proposed couplings. Through analytical calculations, we were conscious of the negative and positive contribution of the new charged boson and vector respectively, potentially benefiting to tackle the electron and muon $g-2$ puzzle. Nevertheless, Michel parameters derived from polarized muon decay, which plays a critical role in elucidating the chirality effects foreseen by the theory, through these above analyses, we have delineated a boundary for new couplings based on a 2 $\sigma$ experimental uncertainty. A key finding of this research is the realization that universal coupling assumptions are insufficient to account for the muon g-2 anomaly. However, by incorporating the concept of coupling non-universality, we uncover a promising pathway to resolve this long-standing anomaly. This approach allows for a significant reduction in one lepton coupling by 2-5 magnitude order and thereby broadens the scope for other couplings. Besides that, the reason for $2\sigma$ consideration in our Michel parameters could give us a hint on NP out of our study approach.

Furthermore, the study extends its implications to the realms of UV models, particularly in estimating the mass scale of the newly charged bosons. These predictions can surpass current experimental bounds, particularly in the LHC searches, if the Michel parameters' experiment uncertainty is strictly upgraded. Finally, in addressing the Zee Model, we have also established a strong constraint on the feasible parameter space of Yukawa couplings, and after a rough estimation, it possibly closes the door to provide the answer to the neutrino oscillation puzzle under $1\sigma$ uncertainty of Michel parameters considered. The comprehensive and robust numerical parameter scan is being in process.

Looking forward, the framework and findings of this study offer a rich ground for theoretical development in particle physics. The theoretical advancements made here should be considered as a stepping stone towards more comprehensive models that can integrate these new bosons into the broader understanding of particle interactions. Moreover, studying the muon g-2 anomaly opens up new avenues for theoretical and experimental physicists alike to explore variations in coupling strengths and their impact on other physical phenomena. Further experimental investigations will be crucial in validating the predictions made in this study and in searching for direct or indirect evidence of the new charged bosons and the unique interactions they entail.

# Chapter 8

# Appendix

## 8.1 $L \to l\gamma$ form factor

### 8.1.1 Charged vector form factors



1. **Diagram a**

   - Dirac form factor

$$
\begin{aligned}
F_1^{V,a} = \frac{-eQ_V}{2m_V^2} \Bigg\{ & 3\left(V_{ik}^R V_{jk}^{*L} + V_{ik}^L V_{jk}^{*R}\right)(m_1+m_2)\, m_k m_V^2 \sum_{i=0}^{2} C_i^{V,a} + \\
& \left(V_{ik}^L V_{jk}^{*L} + V_{ik}^R V_{jk}^{*R}\right) \Bigg[ \sum_{i=1}^{2} \left( \frac{m_1^3 m_2^3}{m_i^2} + m_V^2 \left(2m_1 m_2 + m_i^2 + 3\frac{m_1^2 m_2^2}{m_i^2}\right) - m_1^2 m_2^2 \right) C_i^{V,a} - \\
& \sum_{i,j=1}^{2} \left( \frac{m_1^4 m_2^4}{m_i^4} - 3\frac{m_1^3 m_2^3}{m_i^2} - m_V^2 \left(2m_1 m_2 + 4\frac{m_1^2 m_2^2}{m_i^2}\right) + 2m_1^2 m_2^2 \right) C_{ij}^{V,a} - \\
& 2\left(m_1^2 + m_2^2 + 5m_1 m_2 - 6m_V^2\right) C_{00}^{V,a} - 6\sum_{i=1}^{2} \left( 2\frac{m_1^2 m_2^2}{m_i^2} - 3m_1 m_2 + m_i^2 \right) C_{00i}^{V,a} - \\
& \sum_{i,j,k=1}^{2} \left( m_1^4 m_2^4 \left( \frac{1}{m_i^4} + \frac{1}{m_j^2 m_k^2} \right) - 3\frac{m_1^3 m_2^3}{m_i^2} + m_1^2 m_2^2 \right) C_{ijk}^{V,a} - \sum_{i,j=1}^{2} \left( 14\frac{m_1^2 m_2^2}{m_i^2} - 8m_1 m_2 \right) C_{00ij}^{V,a} - \\
& \sum_{i,j,k,l=1}^{2} \left( 2\frac{m_1^4 m_2^4}{m_i^2 m_j^2} - \frac{m_1^3 m_2^3}{m_i^2} \right) C_{ijkl}^{V,a} - \frac{\left(2m_1^2 - 7m_1 m_2 + 2m_2^2 - 6m_k^2 - 4m_V^2\right)^2}{4} \Bigg] \Bigg\}.
\end{aligned}
\tag{8.1}
$$

   - Anapole form factor

$$G_1^{V,a} = \frac{-eQ_V}{2m_V^2}\left\{3\left(V_{ik}^R V_{jk}^{*L} - V_{ik}^L V_{jk}^{*R}\right)(m_1-m_2)\, m_k m_V^2 \sum_{i=0}^{2} C_i^{V,a} + \right.$$

$$\left(V_{ik}^R V_{jk}^{*R} - V_{ik}^L V_{jk}^{*L}\right)\left[\sum_{i=1}^{2}\left(\frac{m_1^3 m_2^3}{m_i^2} + m_V^2\left(2m_1m_2 - m_i^2 - 3\frac{m_1^2 m_2^2}{m_i^2}\right) + m_1^2 m_2^2\right) C_i^{V,a} + \right.$$

$$\sum_{i,j=1}^{2}\left(\frac{m_1^4 m_2^4}{m_i^4} + 3\frac{m_1^3 m_2^3}{m_i^2} - m_V^2\left(4\frac{m_1^2 m_2^2}{m_i^2} - 2m_1m_2\right) + 2m_1^2 m_2^2\right) C_{ij}^{V,a} +$$

$$2\left(m_1^2 + m_2^2 + 5m_1m_2 - 6m_V^2\right) C_{00}^{V,a} + 6\sum_{i=1}^{2}\left(2\frac{m_1^2 m_2^2}{m_i^2} + 3m_1m_2 + m_i^2\right) C_{00i}^{V,a} +$$

$$\sum_{i,j,k=1}^{2}\left(m_1^4 m_2^4\left(\frac{1}{m_i^4} + \frac{1}{m_j^2 m_k^2}\right) + 3\frac{m_1^3 m_2^3}{m_i^2} + m_1^2 m_2^2\right) C_{ijk}^{V,a} + \sum_{i,j=1}^{2}\left(14\frac{m_1^2 m_2^2}{m_i^2} + 8m_1m_2\right) C_{00ij}^{V,a} +$$

$$\left.\left.\sum_{i,j,k,l=1}^{2}\left(2\frac{m_1^4 m_2^4}{m_i^2 m_j^2} + \frac{m_1^3 m_2^3}{m_i^2}\right) C_{ijkl}^{V,a} + \frac{\left(2m_1^2 - m_1m_2 + 2m_2^2 - 6m_k^2 - 4m_V^2\right)^2}{4}\right]\right\}. \tag{8.2}$$

- MDM form factor

$$F_2^{V,a} = \frac{-eQ_V}{4m_V^2}\left\{\left(V_{ik}^R V_{jk}^{*L} + V_{ik}^L V_{jk}^{*R}\right) m_k \left[\left(m_1^2 + m_2^2 - 4m_V^2\right) C_0^{V,a} + \right.\right.$$

$$\left.\sum_{i=1}^{2}\left(3\frac{m_1^2 m_2^2}{m_i^2} + m_i^2 - 6m_V^2\right) C_i^{V,a} + 8C_{00}^{V,a} + 2\sum_{i,j=1}^{2}\frac{m_1^2 m_2^2}{m_i^2} C_{ij}^{V,a} - 1\right] -$$

$$\left(V_{ik}^L V_{jk}^{*L} + V_{ik}^R V_{jk}^{*R}\right)\left[\sum_{i=1}^{2}\left(\frac{m_1^3 m_2^3}{m_i^3} - m_1m_2m_i + 2m_V^2\frac{m_1m_2}{m_i}\right) C_i^{V,a} + 8(m_1+m_2)\, C_{00}^{V,a} + \right.$$

$$\sum_{i,j=1}^{2}\left(\frac{m_1^3 m_2^3}{m_i^3} + 2\frac{m_1^3 m_2^3}{m_i m_j^2} - m_1m_2m_i + 4m_V^2\frac{m_1m_2}{m_i}\right) C_{ij}^{V,a} + 24\sum_{i=1}^{2}\frac{m_1m_2}{m_i} C_{00i}^{V,a} +$$

$$\left.\left. 4\sum_{i,j,k=1}^{2}\frac{m_1^3 m_2^3}{m_i m_j^2} C_{ijk}^{V,a} + 2\sum_{i,j,k,l=1}^{2}\frac{m_1^3 m_2^3}{m_i m_j^2} C_{ijkl}^{V,a} + 16\sum_{i,j=1}^{2}\frac{m_1m_2}{m_i} C_{00ij}^{V,a} - \frac{7}{12}(m_1+m_2)\right]\right\} -$$

$$\frac{aeQ_V}{4m_V^2}\left\{\left(V_{ik}^L V_{jk}^{*L} + V_{ik}^R V_{jk}^{*R}\right)(m_1+m_2)\left[\sum_{i=1}^{2}\left(\frac{m_1^2 m_2^2}{m_i^2} - m_1m_2 + 2m_V^2\right) C_i^{V,a} + 4C_{00}^{V,a} + \right.\right.$$

$$\left.\sum_{i,j=1}^{2}\left(\frac{m_1^2 m_2^2}{m_i^2} - m_1m_2\right) C_{ij}^{V,a}\right] - \left(V_{ik}^R V_{jk}^{*L} + V_{ik}^L V_{jk}^{*R}\right) m_k \left[\left((m_1-m_2)^2 - 4m_V^2\right) C_0^{V,a} + \right.$$

$$\left.\left.\sum_{i=1}^{2}\frac{\left(m_1m_2 - m_i^2\right)\left(3m_1m_2 - m_i^2\right)}{m_i^2} C_i^{V,a} + 8C_{00}^{V,a} + 2\sum_{i,j=1}^{2}\left(\frac{m_1^2 m_2^2}{m_i^2} - m_1m_2\right) C_{ij}^{V,a}\right]\right\}. \tag{8.3}$$

- EDM form factor

$$G_2^{V,a}=\frac{-eQ_V}{4m_V^2}\Big\{\left(V_{ik}^LV_{jk}^{*R}-V_{ik}^RV_{jk}^{*L}\right)m_k\Big[\left(m_1^2+m_2^2-4m_V^2\right)C_0^{V,a}+$$

$$\sum_{i=1}^{2}\left(3\frac{m_1^2m_2^2}{m_i^2}+m_i^2-6m_V^2\right)C_i^{V,a}+8C_{00}^{V,a}+2\sum_{i,j=1}^{2}\frac{m_1^2m_2^2}{m_i^2}C_{ij}^{V,a}-1\Big]+$$

$$\left(V_{ik}^LV_{jk}^{*L}-V_{ik}^RV_{jk}^{*R}\right)\Big[\sum_{i=1}^{2}(-1)^i\left(\frac{m_1^3m_2^3}{m_i^3}-m_1m_2m_i+2m_V^2\frac{m_1m_2}{m_i}\right)C_i^{V,a}+8\left(m_1-m_2\right)C_{00}^{V,a}+$$

$$\sum_{i,j=1}^{2}(-1)^i\left(\frac{m_1^3m_2^3}{m_i^3}+2\frac{m_1^3m_2^3}{m_im_j^2}-m_1m_2m_i+4m_V^2\frac{m_1m_2}{m_i}\right)C_{ij}^{V,a}+24\sum_{i=1}^{2}(-1)^i\frac{m_1m_2}{m_i}C_{00i}^{V,a}+$$

$$2\sum_{i,j,k,l=1}^{2}(-1)^i\frac{m_1^3m_2^3}{m_im_j^2}\left(C_{ijk}^{V,a}+C_{ijkl}^{V,a}\right)+16\sum_{i,j=1}^{2}(-1)^i\frac{m_1m_2}{m_i}C_{00ij}^{V,a}-\frac{7}{12}\left(m_1-m_2\right)\Big]\Big\}-$$

$$\frac{aeQ_V}{4m_V^2}\Big\{\left(V_{ik}^RV_{jk}^{*R}-V_{ik}^LV_{jk}^{*L}\right)\left(m_1-m_2\right)\Big[\sum_{i=1}^{2}\left(\frac{m_1^2m_2^2}{m_i^2}+m_1m_2+2m_V^2\right)C_i^{V,a}+4C_{00}^{V,a}+$$

$$\sum_{i,j=1}^{2}\left(\frac{m_1^2m_2^2}{m_i^2}+m_1m_2\right)C_{ij}^{V,a}\Big]+\left(V_{ik}^RV_{jk}^{*L}-V_{ik}^LV_{jk}^{*R}\right)m_k\Big[\left((m_1+m_2)^2-4m_V^2\right)C_0^{V,a}+$$

$$\sum_{i=1}^{2}\frac{\left(m_1m_2+m_i^2\right)\left(3m_1m_2+m_i^2\right)}{m_i^2}C_i^{V,a}+8C_{00}^{V,a}+2\sum_{i,j=1}^{2}\left(\frac{m_1^2m_2^2}{m_i^2}+m_1m_2\right)C_{ij}^{V,a}\Big]\Big\}. \tag{8.4}$$

As being showed above, only $F_2^{V,a}$ and $G_2^{V,a}$ get contribution from $ieQ_VaF^{\mu\nu}V_\mu^+V_\nu^-$ which corresponds to the tree-level magnetic dipole moment, and for renormalization $F_2^{V,a}, G_2^{V,a}$, set $a=1$.

2. **Diagram b**

   - Dirac form factor

$$F_1^{V,b}=\frac{eQ_l}{2(m_1-m_2)m_V^2}\Big\{\left(V_{ik}^RV_{jk}^{*L}+V_{ik}^LV_{jk}^{*R}\right)m_k\Big[\left(m_1^2-4m_V^2\right)B_0^{V,b}+2m_1^2B_1^{V,b}+$$

$$m_1^2B_{11}^{V,b}+4B_{00}^{V,b}+\frac{1}{6}\left(m_1^2-3m_k^2+15m_V^2\right)\Big]-\left(V_{ik}^LV_{jk}^{*L}+V_{ik}^RV_{jk}^{*R}\right)m_1\Big[\left(m_1^2+2m_V^2\right)B_1^{V,b}+$$

$$2m_1^2B_{11}^{V,b}+m_1^2B_{111}^{V,b}+8B_{00}^{V,b}+6B_{001}^{V,b}+\frac{1}{12}\left(3m_1^2-10m_k^2+4m_V^2\right)\Big]\Big\}. \tag{8.5}$$

   - Anapole form factor

$$G_1^{V,b} = \frac{eQ_l}{2(m_1+m_2)m_V^2}\left\{\left(V_{ik}^{R}V_{jk}^{*L} - V_{ik}^{L}V_{jk}^{*R}\right) m_k \left[\left(m_1^2 - 4m_V^2\right) B_0^{V,b} + 2m_1^2 B_1^{V,b} + \right.\right.$$
$$\left. m_1^2 B_{11}^{V,b} + 4B_{00}^{V,b} + \frac{1}{6}\left(m_1^2 - 3m_k^2 + 15m_V^2\right)\right] - \left(V_{ik}^{L}V_{jk}^{*L} - V_{ik}^{R}V_{jk}^{*R}\right) m_1 \left[\left(m_1^2 + 2m_V^2\right) B_1^{V,b} + \right.$$
$$\left.\left. 2m_1^2 B_{11}^{V,b} + m_1^2 B_{111}^{V,b} + 8B_{00}^{V,b} + 6B_{001}^{V,b} + \frac{1}{12}\left(3m_1^2 - 10m_k^2 + 4m_V^2\right)\right]\right\}. \tag{8.6}$$

3. **Diagram c**

- Dirac form factor

$$F_1^{V,c} = \frac{eQ_l}{2(m_2-m_1)m_V^2}\left\{\left(V_{ik}^{R}V_{jk}^{*L} + V_{ik}^{L}V_{jk}^{*R}\right) m_k \left[\left(m_2^2 - 4m_V^2\right) B_0^{V,c} + 2m_2^2 B_1^{V,c} + \right.\right.$$
$$\left. m_2^2 B_{11}^{V,c} + 4B_{00}^{V,c} + \frac{1}{6}\left(m_2^2 - 3m_k^2 + 15m_V^2\right)\right] - \left(V_{ik}^{L}V_{jk}^{*L} + V_{ik}^{R}V_{jk}^{*R}\right) m_2 \left[\left(m_2^2 + 2m_V^2\right) B_1^{V,c} + \right.$$
$$\left.\left. 2m_2^2 B_{11}^{V,c} + m_2^2 B_{111}^{V,c} + 8B_{00}^{V,c} + 6B_{001}^{V,c} + \frac{1}{12}\left(3m_2^2 - 10m_k^2 + 4m_V^2\right)\right]\right\}. \tag{8.7}$$

- Anapole form factor

$$G_1^{V,c} = \frac{-eQ_l}{2(m_2+m_1)m_V^2}\left\{\left(V_{ik}^{R}V_{jk}^{*L} - V_{ik}^{L}V_{jk}^{*R}\right) m_k \left[\left(m_2^2 - 4m_V^2\right) B_0^{V,c} + 2m_2^2 B_1^{V,c} + \right.\right.$$
$$\left. m_2^2 B_{11}^{V,c} + 4B_{00}^{V,c} + \frac{1}{6}\left(m_2^2 - 3m_k^2 + 15m_V^2\right)\right] + \left(V_{ik}^{L}V_{jk}^{*L} - V_{ik}^{R}V_{jk}^{*R}\right) m_2 \left[\left(m_2^2 + 2m_V^2\right) B_1^{V,c} + \right.$$
$$\left.\left. 2m_2^2 B_{11}^{V,c} + m_2^2 B_{111}^{V,c} + 8B_{00}^{V,c} + 6B_{001}^{V,c} + \frac{1}{12}\left(3m_2^2 - 10m_k^2 + 4m_V^2\right)\right]\right\}. \tag{8.8}$$

4. **Diagram d**

- Dirac form factor

$$F_1^{V,d} = \frac{eQ_k}{2m_V^2}\left\{\left(V_{ik}^R V_{jk}^{*L} + V_{ik}^L V_{jk}^{*R}\right)(m_1+m_2)\, m_k \left[-4m_V^2 \sum_{i=0}^{2} C_i^{V,d} + 4C_{00}^{V,d} + 6\sum_{i=1}^{2} C_{00i}^{V,d} + \right.\right.$$
$$\sum_{i,j=1}^{2} \frac{m_1^2 m_2^2}{m_i^2}\left(C_{ij}^{V,d} + \sum_{k=1}^{2} C_{ijk}^{V,d}\right) - \left.\frac{1}{6}\right] + \left(V_{ik}^L V_{jk}^{*L} + V_{ik}^R V_{jk}^{*R}\right)\left[\frac{1}{24}\left(7m_1^2 + 7m_2^2 + 12m_1m_2 - \right.\right.$$
$$\left. 28m_k^2 + 28m_V^2\right) + 2m_V^2 \sum_{i=0}^{2}\left(\frac{(i-1)(i-2)}{2}\left(m_k^2 - m_1m_2\right) + 2m_1m_2\right) C_i^{V,d} -$$
$$2\left(m_1m_2 + m_k^2 + 2m_V^2\right) C_{00}^{V,d} + 12\sum_{i=1}^{2}\frac{m_1^2m_2^2}{m_i^2}\left(C_{00i}^{V,d} + \sum_{j=1}^{2} C_{00ij}^{V,d}\right) +$$
$$\left.\left.\sum_{i,j=1}^{2}\left[m_1m_2\left(m_k^2 + 2m_V^2\right) + \frac{m_1^4m_2^4}{m_i^2m_j^2} + \right] C_{ij}^{V,d} + \sum_{i,j,k=1}^{2}\frac{m_1^4m_2^4}{m_i^2m_j^2}\left(C_{ijk}^{V,d} + \sum_{l=1}^{2} C_{ijkl}^{V,d}\right) + 24C_{0000}^{V,d}\right]\right\}. \tag{8.9}$$

- Anapole form factor

$$G_1^{V,d} = \frac{eQ_k}{2m_V^2}\left\{\left(V_{ik}^R V_{jk}^{*L} - V_{ik}^L V_{jk}^{*R}\right)(m_1-m_2)\, m_k \left[-4m_V^2 \sum_{i=0}^{2} C_i^{V,d} + 4C_{00}^{V,d} + 6\sum_{i=1}^{2} C_{00i}^{V,d} + \right.\right.$$
$$\sum_{i,j=1}^{2} \frac{m_1^2 m_2^2}{m_i^2}\left(C_{ij}^{V,d} + \sum_{k=1}^{2} C_{ijk}^{V,d}\right) - \left.\frac{1}{6}\right] + \left(V_{ik}^R V_{jk}^{*R} - V_{ik}^L V_{jk}^{*L}\right)\left[\frac{1}{24}\left(-3m_1^2 - 3m_2^2 + \right.\right.$$
$$\left. 12m_1m_2 + 28m_k^2 - 28m_V^2\right) + 2m_V^2 \sum_{i=0}^{2}\left(\frac{(1-i)(i-2)}{2}\left(m_k^2 + m_1m_2\right) + 2m_1m_2\right) C_i^{V,d} +$$
$$2\left(-m_1m_2 + m_k^2 + 2m_V^2\right) C_{00}^{V,d} - 12\sum_{i=1}^{2}\frac{m_1^2m_2^2}{m_i^2}\left(C_{00i}^{V,d} + \sum_{j=1}^{2} C_{00ij}^{V,d}\right) +$$
$$\left.\left.\sum_{i,j=1}^{2}\left(m_1m_2\left(m_k^2 + 2m_V^2\right) - \frac{m_1^4m_2^4}{m_i^2m_j^2}\right) C_{ij}^{V,d} - \sum_{i,j,k=1}^{2}\frac{m_1^4m_2^4}{m_i^2m_j^2}\left(C_{ijk}^{V,d} + \sum_{l=1}^{2} C_{ijkl}^{V,d}\right) - 24C_{0000}^{V,d}\right]\right\}. \tag{8.10}$$

- MDM form factor

$$F_2^{V,d} = \frac{eQ_k}{2m_V^2}\left\{\left(V_{ik}^R V_{jk}^{*L} + V_{ik}^L V_{jk}^{*R}\right) m_k \left[4m_V^2 \sum_{i=0}^{2} C_i^{V,d} + 4C_{00}^{V,d} + \sum_{ij=1}^{2}\left(m_1m_2 - \frac{m_1^2m_2^2}{m_i^2}\right) C_{ij}^{V,d} - \right.\right.$$
$$6\sum_{i=1}^{2} C_{00i}^{V,d} - \sum_{i,j,k=1}^{2}\frac{m_1^2m_2^2}{m_i^2} C_{ijk}^{V,d} - \left.\frac{1}{3}\right] + \left(V_{ik}^L V_{jk}^{*L} + V_{ik}^R V_{jk}^{*R}\right)\left[-m_V^2 \sum_{i=1}^{2}\left(4\frac{m_1m_2}{m_i} + 2m_i\right) C_i^{V,d} - \right.$$
$$2m_V^2\left(m_1+m_2\right) C_0^{V,d} + \sum_{i,j=1}^{2}\left(-\frac{m_1m_2}{m_i}\left(m_k^2 + 2m_V^2\right) + \frac{m_1^2m_2^2}{m_i^2} m_j\right) C_{ij}^{V,d} + 2(m_1+m_2) C_{00}^{V,d} +$$
$$\left.\left.\sum_{i,j,k=1}^{2}\frac{m_1^2m_2^2}{m_j^2} m_i C_{ijk}^{V,d} + 6\sum_{i=1}^{2} m_i C_{00i}^{V,d} + \frac{m_1+m_2}{6}\right]\right\}. \tag{8.11}$$

- EDM form factor

$$G_2^{V,d} = \frac{eQ_k}{2m_V^2}\left\{\left(V_{ik}^L V_{jk}^{*R} - V_{ik}^R V_{jk}^{*L}\right) m_k \left[4m_V^2 \sum_{i=0}^{2} C_i^{V,d} - 4C_{00}^{V,d} + \sum_{ij=1}^{2}\left(m_1 m_2 - \frac{m_1^2 m_2^2}{m_i^2}\right) C_{ij}^{V,d} - 6\sum_{i=1}^{2} C_{00i}^{V,d} + \sum_{i,j,k=1}^{2} \frac{m_1^2 m_2^2}{m_i^2} C_{ijk}^{V,d} + \frac{1}{3}\right] + \left(V_{ik}^R V_{jk}^{*R} - V_{ik}^L V_{jk}^{*L}\right)\left[-m_V^2 \sum_{i=1}^{2}\left(4\frac{m_1 m_2}{m_i} - 2m_i\right) C_i^{V,d} - 2m_V^2\left(m_1 - m_2\right) C_0^{V,d} - \sum_{i,j=1}^{2}(-1)^i\left(\frac{m_1 m_2}{m_i}\left(m_k^2 + 2m_V^2\right) + \frac{m_1^2 m_2^2}{m_i^2} m_j\right) C_{ij}^{V,d} + 2(m_1 - m_2) C_{00}^{V,d} - \sum_{i,j,k=1}^{2}(-1)^i \frac{m_1^2 m_2^2}{m_j^2} m_i C_{ijk}^{V,d} - 6\sum_{i=1}^{2}(-1)^i m_i C_{00i}^{V,d} + \frac{m_1 - m_2}{6}\right]\right\}. \tag{8.12}$$

### 8.1.2 Charged scalar form factor

1. **Diagram a**

- Dirac form factor

$$F_1^{\phi,a} = \frac{eQ_\phi}{2}\left\{\left(Y_{ik}^R Y_{jk}^{*L} + Y_{ik}^L Y_{jk}^{*R}\right)(m_1 + m_2) m_k \sum_{i=0}^{2} C_i^{\phi,a} - \left(Y_{ik}^L Y_{jk}^{*L} + Y_{ik}^R Y_{jk}^{*R}\right)\left[(m_1 + m_2)\sum_{i,j=1}^{2}\frac{m_1 m_2}{m_i}\left(\frac{C_i^{\phi,a}}{2} + C_{ij}^{\phi,a}\right) + 2C_{00}^{\phi,a}\right]\right\}. \tag{8.13}$$

- Anapole form factor

$$G_1^{\phi,a} = \frac{eQ_\phi}{2}\left\{\left(Y_{ik}^L Y_{jk}^{*R} - Y_{ik}^R Y_{jk}^{*L}\right)(m_1 - m_2) m_k \sum_{i=0}^{2} C_i^{\phi,a} + \left(Y_{ik}^L Y_{jk}^{*L} - Y_{ik}^R Y_{jk}^{*R}\right)\left[\sum_{i,j=1}^{2}\left(\frac{m_1^2 m_2^2}{m_i^2} - m_1 m_2\right)\left(\frac{C_i^{\phi,a}}{2} + C_{ij}^{\phi,a}\right) + 2C_{00}^{\phi,a}\right]\right\}. \tag{8.14}$$

- MDM form factor

$$F_2^{\phi,a} = \frac{eQ_\phi}{2}\left[\left(Y_{ik}^L Y_{jk}^{*L} + Y_{ik}^R Y_{jk}^{*R}\right)\sum_{i,j=1}^{2}\frac{m_1 m_2}{m_i}\left(\frac{C_i^{\phi,a}}{2} + C_{ij}^{\phi,a}\right) - \cdot\left(Y_{ik}^R Y_{jk}^{*L} + Y_{ik}^L Y_{jk}^{*R}\right) m_k \sum_{i=0}^{2} C_i^{\phi,a}\right]. \tag{8.15}$$

- EDM form factor

$$G_2^{\phi,a} = \frac{eQ_\phi}{2}\left[\left(Y_{ik}^{L}Y_{jk}^{*L} - Y_{ik}^{R}Y_{jk}^{*R}\right)\sum_{i,j=1}^{2}(-1)^i\frac{m_1 m_2}{m_i}\left(\frac{C_i^{\phi,a}}{2} + C_{ij}^{\phi,a}\right) + \right.$$
$$\left.\left(Y_{ik}^{L}Y_{jk}^{*R} - Y_{ik}^{R}Y_{jk}^{*L}\right) m_k \sum_{i=0}^{2} C_i^{\phi,a}\right]. \tag{8.16}$$

2. **Diagram b**

 • Dirac form factor

$$F_1^{\phi,b} = \frac{eQ_l}{2(m_1 - m_2)}\left[m_k\left(Y_{ik}^{R}Y_{jk}^{*L} + Y_{ik}^{L}Y_{jk}^{*R}\right)B_0^{\phi,b} - m_1\left(Y_{ik}^{L}Y_{jk}^{*L} + Y_{ik}^{R}Y_{jk}^{*R}\right)B_1^{\phi,b}\right]. \tag{8.17}$$

 • Anapole form factor

$$G_1^{\phi,b} = \frac{-eQ_l}{2(m_1 + m_2)}\left[m_k\left(Y_{ik}^{R}Y_{jk}^{*L} - Y_{ik}^{L}Y_{jk}^{*R}\right)B_0^{\phi,b} - m_1\left(Y_{ik}^{L}Y_{jk}^{*L} - Y_{ik}^{R}Y_{jk}^{*R}\right)B_1^{\phi,b}\right]. \tag{8.18}$$

3. **Diagram c**

 • Dirac form factor

$$F_1^{\phi,c} = \frac{-e}{2(m_2 - m_1)}\left[m_k\left(Y_{ik}^{R}Y_{jk}^{*L} + Y_{ik}^{L}Y_{jk}^{*R}\right)B_0^{\phi,c} - m_2\left(Y_{ik}^{L}Y_{jk}^{*L} + Y_{ik}^{R}Y_{jk}^{*R}\right)B_1^{\phi,c}\right]. \tag{8.19}$$

 • Anapole form factor

$$G_1^{\phi,c} = \frac{-e}{2(m_2 + m_1)}\left[m_k\left(Y_{ik}^{R}Y_{jk}^{*L} - Y_{ik}^{L}Y_{jk}^{*R}\right)B_0^{\phi,c} + m_2\left(Y_{ik}^{L}Y_{jk}^{*L} - Y_{ik}^{R}Y_{jk}^{*R}\right)B_1^{\phi,c}\right]. \tag{8.20}$$

4. **Diagram d**

 • Dirac form factor

$$F_1^{\phi,d} = \frac{eQ_k}{2}\left\{\left(Y_{ik}^{R}Y_{jk}^{*L} + Y_{ik}^{L}Y_{jk}^{*R}\right)(m_1 + m_2)\, m_k \sum_{i=0}^{2} C_i^{\phi,d} + \right.$$
$$\left.\left(Y_{ik}^{L}Y_{jk}^{*L} + Y_{ik}^{R}Y_{jk}^{*R}\right)\left[\left(m_1 m_2 + m_k^2\right)C_0^{\phi,d} + m_1 m_2 \sum_{i,j=1}^{2}\left(C_i^{\phi,d} + C_{ij}^{\phi,d}\right) - 2C_{00}^{\phi,d} + \frac{1}{2}\right]\right\}. \tag{8.21}$$

- Anapole form factor

$$G_1^{\phi,d} = \frac{eQ_k}{2}\left\{\left(Y_{ik}^L Y_{jk}^{*R} - Y_{ik}^R Y_{jk}^{*L}\right)(m_1 - m_2)\, m_k \sum_{i=0}^{2} C_i^{\phi,d} + \right.$$
$$\left.\left(Y_{ik}^R Y_{jk}^{*R} - Y_{ik}^L Y_{jk}^{*L}\right)\left[\left(m_k^2 - m_1 m_2\right) C_0^{\phi,d} - m_1 m_2 \sum_{i,j=1}^{2}\left(C_i^{\phi,d} + C_{ij}^{\phi,d}\right) - 2C_{00}^{\phi,d} + \frac{1}{2}\right]\right\}. \tag{8.22}$$

- MDM form factor

$$\begin{aligned} F_2^{\phi,d} = \frac{-eQ_k}{2}\Bigg[&\left(Y_{ik}^L Y_{jk}^{*L} + Y_{ik}^R Y_{jk}^{*R}\right)\sum_{i,j=1}^{2}\frac{m_1 m_2}{m_i}\left(\frac{C_i^{\phi,d}}{2} + C_{ij}^{\phi,d}\right) + \\ &\left(Y_{ik}^R Y_{jk}^{*L} + Y_{ik}^L Y_{jk}^{*R}\right) m_k \sum_{i=1}^{2} C_i^{\phi,d}\Bigg]. \end{aligned} \tag{8.23}$$

- EDM form factor

$$\begin{aligned} G_2^{\phi,d} = \frac{-eQ_k}{2}\Bigg[&\left(-Y_{ik}^L Y_{jk}^{*L} - Y_{ik}^R Y_{jk}^{*R}\right)\sum_{i,j=1}^{2}(-1)^i\frac{m_1 m_2}{m_i}\left(\frac{C_i^{\phi,d}}{2} + C_{ij}^{\phi,d}\right) + \\ &\left(Y_{ik}^R Y_{jk}^{*L} - Y_{ik}^L Y_{jk}^{*R}\right) m_k \sum_{i=1}^{2} C_i^{\phi,d}\Bigg]. \end{aligned} \tag{8.24}$$

## 8.2 Fierz transformation

Fierz transformation is a mathematical tool used in quantum field theory and particle physics to rearrange or transform complex field operator's products into a more manageable form. This rearrangement is particularly useful when dealing with four-fermion interactions. Its core transformation is the Fierz identity. This identity allows the rearrangement of bilinear products of spinor fields. A bilinear product involves two spinor fields and gamma matrices. The Fierz identity expresses a product of two such bilinears in terms of a sum of bilinears with the spinor fields rearranged. In this study, the Fierz identity is formulated for the set of gamma matrices $\{\Gamma_S = 1, \Gamma_V = \gamma_\mu, \Gamma_T = \sigma_{\mu\nu}, \Gamma_A = \gamma_\mu\gamma_5, \Gamma_P = \gamma_5\}$.

$$\sum_\alpha g_\alpha \bar{\psi}_i \Gamma_\alpha \psi_j \bar{\psi}_m \Gamma_\alpha \psi_n = \sum_\beta \tilde{g}_\beta \bar{\psi}_i \Gamma_\beta \psi_n \bar{\psi}_m \Gamma_\beta \psi_j \tag{8.25}$$

by a transformation matrix between $g_\alpha$ and $\tilde{g}_\beta$ that one can read off for $\alpha, \beta$ running over the set $\{S, V, T, A, P\}$

$$\begin{bmatrix} \tilde{g}_S \\ \tilde{g}_V \\ \tilde{g}_T \\ \tilde{g}_A \\ \tilde{g}_P \end{bmatrix} = \frac{1}{4} \begin{pmatrix} 1 & 4 & 12 & -4 & 1 \\ 1 & -2 & 0 & -2 & -1 \\ \frac{1}{2} & 0 & -2 & 0 & \frac{1}{2} \\ -1 & -2 & 0 & -2 & 1 \\ 1 & -4 & 12 & 4 & 1 \end{pmatrix} \begin{bmatrix} g_S \\ g_V \\ g_T \\ g_A \\ g_P \end{bmatrix} \tag{8.26}$$

where $i, j, m, n$ are flavor indices.

## 8.3 Full massive Lorenz index two-body phase pace

# Bibliography


[1] L. Michel, *Interaction between four half spin particles and the decay of the $\mu$ meson*, *Proc. Phys. Soc. A* **63** (1950) 514.

[2] T. Kinoshita and A. Sirlin, *Polarization of electrons in muon decay with general parity-nonconserving interactions*, *Phys. Rev.* **108** (1957) 844.

[3] M. Steinhauser, *Übungen zu strahlungskorrekturen in eichtheorien, II. Institut für Theoretische Physik, Universität Hamburg, 22761 Hamburg* (2003) .

[4] C. Bouchiat and L. Michel, *Theory of $\mu$-meson decay with the hypothesis of nonconservation of parity*, *Phys. Rev.* **106** (1957) 170.

[5] T. Kinoshita and A. Sirlin, *Muon decay with parity nonconserving interactions and radiative corrections in the two-component theory*, *Phys. Rev.* **107** (1957) 593.

[6] A. Crivellin, M. Hoferichter and C. A. Manzari, *Fermi constant from muon decay versus electroweak fits and cabibbo-kobayashi-maskawa unitarity*, *Physical Review Letters* **127** (2021) .

[7] T. D. Lee and C. N. Yang, *Theory of charged vector mesons interacting with the electromagnetic field*, *Phys. Rev.* **128** (1962) 885.

[8] W. J. Marciano, *Fermi constants and "new physics"*, *Physical Review D* **60** (1999) .

[9] Muon g-2 Collaboration collaboration, *Final report of the e821 muon anomalous magnetic moment measurement at bnl*, *Phys. Rev. D* **73** (2006) 072003.

[10] T. Aoyama, T. Kinoshita and M. Nio, *Theory of the Anomalous Magnetic Moment of the Electron*, *Atoms* **7** (2019) 28.